

THE PLATINUM-GROUP MINERALS IN THE UPPER SECTION OF THE KEIVITSANSARVI Ni–Cu–PGE DEPOSIT, NORTHERN FINLAND

FERNANDO GERVILLA[§]

*Instituto Andaluz de Ciencias de la Tierra (Universidad de Granada – CSIC) and
Departamento de Mineralogía y Petrología, Facultad de Ciencias, E-18002 Granada, Spain*

KARI KOJONEN

Geological Survey of Finland, Betonimiehenkuja 4, FIN-02150 Espoo, Finland

ABSTRACT

The Keivitsansarvi deposit, in northern Finland, is a low-grade dissemination of Ni–Cu sulfides containing 1.3–26.6 g/t PGE. It occurs in the northeastern part of the 2.05 Ga Keivitsa intrusion and is hosted by olivine wehrlite and olivine websterite, metamorphosed at greenschist-facies conditions. The sulfide-mineralized area shows variable bulk S, Ni, Co, Cu, PGE, Au, As, Sb, Se, Te and Bi contents. S and Au tend to decrease irregularly from bottom to top of the deposit, whereas Ni, Ni/Co, PGE, As, Sb, Se, Te and Bi tend to increase. Thus, the upper section of the deposit has low S (<1.5 wt.%) and Au (160 ppb on average), but elevated levels of the PGE (2120 ppb Pt, 1855 ppb Pd on average). Sulfides consist of intergranular, highly disseminated aggregates mainly made up of pentlandite, pyrite, and chalcopyrite (all showing fine intergrowths), as well as nickeline, maucherite and gersdorffite in some samples. Most platinum-group minerals occur as single, minute grains included in silicates (57%) or attached to the grain boundaries of sulfides (36%). Only a few PGM grains (6%) are included in sulfides. Pt minerals (mainly moncheite and sperrylite) are the most abundant PGM, whereas Pd minerals (mainly merenskyite, Pd-rich melonite, kotulskite and sobolevskite) are relatively scarce, and most contain significant amounts of Pt. Whole-rock PGE analyses show a general Pd enrichment with respect to Pt. This discrepancy results from the fact that a major part of Pd is hidden in solid solution in the structure of gersdorffite, nickeline, maucherite and pentlandite. The mineral assemblages and textures of the upper section of the Keivitsansarvi deposit result from the combined effect of serpentinization, hydrothermal alteration and metamorphism of pre-existing, low-grade disseminated Ni–Cu ore formed by the intercumulus crystallization of a small fraction of immiscible sulfide melt. Serpentinization caused Ni enrichment of sulfides and preserved the original PGE concentrations of the magmatic mineralization. Later, coeval with greenschist-facies metamorphism, PGE and some As (together with other semimetals) were leached out from other mineralized zones by hydrothermal fluids, probably transported in the form of chloride complexes, and precipitated in discrete Ni–Cu–PGE-rich horizons, as observed in the upper part of the deposit. Metamorphism also caused partial dissolution and redistribution of the sulfide (and arsenide) aggregates, contributing to a further Ni enrichment in the sulfide ores.

Keywords: nickel–copper ore, platinum-group minerals, palladian bismuthotellurides, Keivitsa intrusion, Finland.

SOMMAIRE

Le gisement de Keivitsansarvi, dans le nord de la Finlande, est une accumulation de sulfures de Ni–Cu disséminés contenant de 1.3 à 26.6 g/t d'éléments du groupe du platine (EGP). Ce gisement se trouve dans le secteur nord-est du complexe de Keivitsa, mis en place il y a 2.05 Ga, et encaissé par une wehrlite à olivine et une websterite à olivine, métamorphosées aux conditions du faciès schistes verts. La fraction sulfurée contient des quantités variables de S, Ni, Co, Cu, EGP, Au, As, Sb, Se, Te et Bi. La teneur en S et en Au tend à diminuer de façon irrégulière du bas vers le haut de la séquence, tandis que la teneur en Ni, EGP, As, Sb, Se, Te et Bi, et la valeur de Ni/Co, tendent à augmenter. La partie supérieure du gisement montre donc de faibles teneurs en S (< 1.5%, poids) et en Au (160 ppb, en moyenne), mais des teneurs élevées en EGP (2120 ppb Pt, 1855 ppb Pd, en moyenne). Les sulfures sont intergranulaires, en fait des aggrégats fortement disséminés contenant surtout pentlandite, pyrite, et chalcopyrite (montrant toutes des intercroissances fines), de même que nickeline, maucherite et gersdorffite dans certains échantillons. La plupart des minéraux du groupe du platine (MGP) se présentent en grains infimes et monophasés inclus dans des silicates (57%) ou rattachés aux bordures des grains de sulfures (36%). Seulement une faible fraction des grains de MGP (6%) sont inclus dans les sulfures. Les minéraux de Pt (surtout moncheite et sperrylite) sont les plus abondants, tandis que les minéraux de Pd (surtout merenskyite, melonite palladifère, kotulskite et sobolevskite) sont relativement rares, et contiennent une proportion importante de

[§] E-mail address: gervilla@goliat.ugr.es

Pt dans la plupart des cas. Toutefois, les roches montrent un enrichissement global en Pd par rapport au Pt. Cette anomalie découle du fait que la plupart du Pd logerait en solution solide dans la structure de la gersdorffite, la nickeline, la maucherite et la pentlandite. Les assemblages de minéraux et leurs textures dans la partie supérieure du gisement de Keivitsansarvi sont le résultat cumulatif de la serpentinisation, de l'altération hydrothermale et du métamorphisme d'un minerai pré-existant disseminé, à faible teneur en Ni–Cu, formé par la cristallisation intercumulus d'une faible fraction de liquide sulfuré immiscible. La serpentinisation a causé un enrichissement en Ni des sulfures et a conservé les teneurs originales en EGP. Plus tard, lors d'un métamorphisme aux conditions du faciès schistes verts, les EGP et une partie de l'arsenic, ainsi que d'autres semi-métaux, furent lessivés de la zone minéralisée par une venue de fluides hydrothermaux, probablement transportés sous forme de complexes chlorurés, et précipités le long d'horizons devenus enrichis en Ni–Cu–EGP, comme c'est le cas vers la partie supérieure du gisement. La recristallisation métamorphique a aussi causé une dissolution partielle et une redistribution des agrégats de sulfures et d'arséniures, contribuant ainsi à un enrichissement accru du minerai sulfuré en nickel.

(Traduit par la Rédaction)

Mots-clés: minerai de nickel–cuivre, minéraux du groupe du platine, bismuthotellurures palladifères, intrusion de Keivitsa, Finlande.

INTRODUCTION

Many early Proterozoic layered intrusions in central Finnish Lapland and in Russian Karelia contain mineralized zones enriched in the platinum-group elements (PGE; Alapieti *et al.* 1990). In some deposits, PGE enrichment is associated with sulfide precipitation during mixing processes between highly differentiated silicate melts and new pulses of primitive mafic–ultramafic melt (*e.g.*, Halkoaho *et al.* 1990a, Huhtelin *et al.* 1990). In other deposits, such enrichment was produced by the precipitation of PGE from fluids or fluid-enriched residual melts that were transported upward through the pile of cumulates (*e.g.*, Halkoaho *et al.* 1990b, Iljina 1994, Barkov *et al.* 1995a, 2001). A third possibility has been proposed by Mutanen *et al.* (1988) and Mutanen (1997), who argued that transport of PGE in the Koitelainen and Keivitsa–Satovaara complexes takes place in the form of melt-soluble Cl complexes and that concentration of PGE occurred by the breakdown of such complexes due to the crystallization of primary, cumulus or postcumulus chlorapatite, Cl-rich hornblende and Cl-rich biotite. Nevertheless, the mineralogy and texture of the PGE-rich upper section of the Keivitsansarvi Ni–Cu deposit, in the Keivitsa intrusion, involve a more complex interpretation, at least combining the effects of magmatic crystallization, serpentinization, hydrothermal alteration and metamorphism.

In this paper, we present the results of a detailed mineralogical and chemical study of selected samples from the upper section of the Keivitsansarvi Ni–Cu–PGE deposit. This study is mainly focused on the mineralogy and mineral chemistry of the PGE and associated sulfide and arsenide assemblages, as well as on the whole-rock distribution of noble metals. Our results lead to an understanding of the distribution of Pt and Pd in the ores, and suggest the existence of discrete, discontinuous PGE-rich horizons (similar to reef-type deposits) at various depths in the upper section of the deposit.

GEOLOGICAL CONTEXT

The Keivitsansarvi Ni–Cu–PGE deposit is located in the northeastern part of the Keivitsa layered intrusion in central Finnish Lapland (Fig. 1). The Keivitsa intrusion occupies a surface area of approximately 16 km² and consists of a lower ultramafic unit (> 2 km thick) overlain by a gabbro unit with a maximum thickness exceeding 500 meters that grades upward into a granophyre unit of variable thickness (a few tens of meters) (Mutanen 1997). The ultramafic unit is composed of pyroxene–olivine cumulates rich in intercumulus plagioclase, containing discontinuous layers and masses of pyroxenite and gabbro. These ultramafic rocks also contain abundant xenoliths of komatiite-related volcanic rocks toward the upper part of the unit, where the Keivitsansarvi deposit is located, and pelitic xenoliths toward the base of the intrusion. The gabbro unit is made up of pyroxene gabbro, ferrogabbro and magnetite gabbro containing discontinuous layers of olivine pyroxenite near the top of the unit, overlying a stratigraphic level rich in pelitic hornfels and minor xenoliths of komatiite. Magnetite gabbro grades upward into a granophyre mainly composed of sodic plagioclase, quartz and secondary hornblende.

The same sequence of cumulate rocks can be observed in the Satovaara intrusion, which is located 2–3 km to the east of the Keivitsa complex (Fig. 1). Mutanen (1997) considered the two bodies as blocks of a single intrusion, the Keivitsa–Satovaara Complex, separated by a NE-trending fault zone.

The parental magma of the Keivitsa–Satovaara complex intruded 2.05 Ga ago (Huhma *et al.* 1995) into a volcanosedimentary sequence slightly above another older (2.44 Ga) and larger (~750 km²) igneous body, the Koitelainen intrusion (Mutanen 1997). The volcanosedimentary sequence mainly consists of komatiite-related flows and tuffs intercalated within a thick sequence of pelitic sedimentary rocks, including

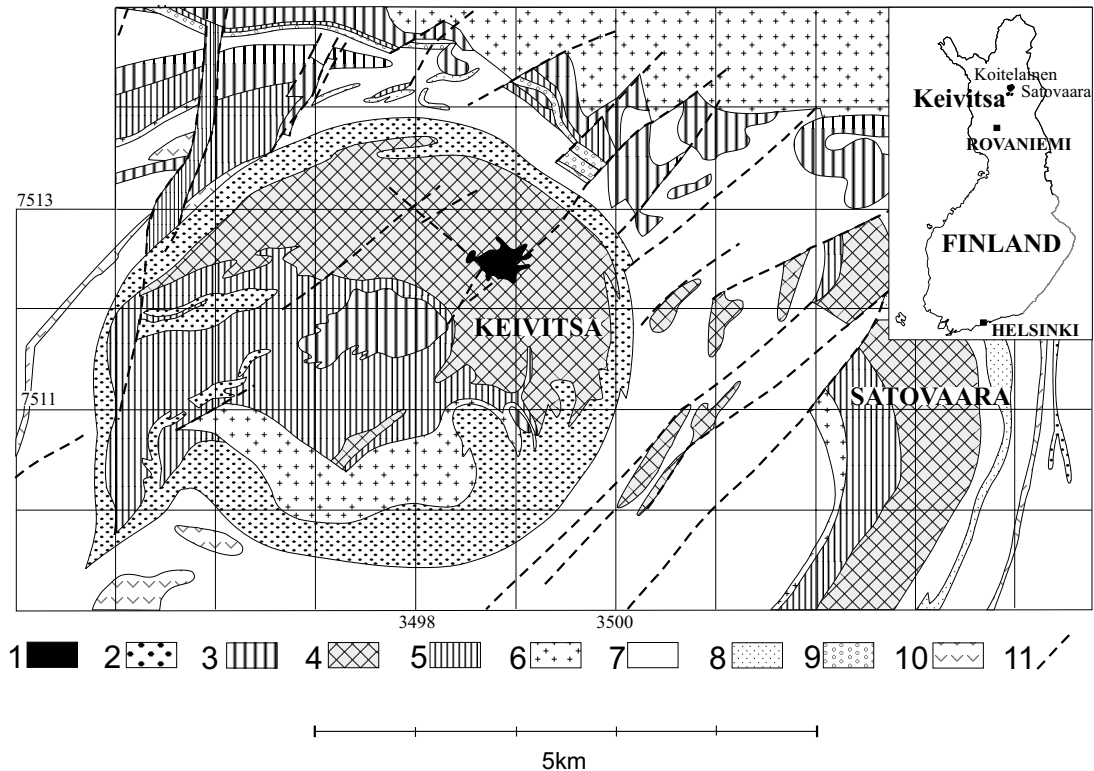


FIG. 1. Simplified geological map of the Keivitsa–Satovaara intrusion, redrawn after Mutanen (1997). The following symbols are shown on the map: 1: Cu–Ni–PGE ore, 2: pelitic and black schist hornfels, 3: komatiite-related ultramafic rocks, 4: olivine wehrlite and olivine websterite, 5: gabbro, 6: granophyre, 7: mica schists and other pelitic rocks, 8: black schists, 9: arkosic quartzite, 10: chlorite–amphibole rocks, 11: fault.

black shales (Fig. 1). These sedimentary rocks contain variable but locally important amounts of graphite and sulfides (especially abundant where the Keivitsa complex was emplaced), and were transformed to hornfels along the contact with the intrusion. Nevertheless, all these rocks (including those of the Keivitsa intrusion) were later metamorphosed (and hydrothermally altered) during a regional metamorphic event that reached greenschist-facies conditions (Tyrväinen 1983).

THE KEIVITSANSARVI DEPOSIT

The host rocks

The Keivitsansarvi deposit occurs in the upper part of the ultramafic unit and is hosted by variably metamorphosed olivine websterite and olivine wehrlite (Fig. 1). According to Mutanen (1997), the unmetamorphosed rocks consist of cumulus augite, olivine, orthopyroxene and magnetite, with intercumulus plagioclase,

phlogopite, hornblende, chlorapatite, monazite, graphite, ilmenite and sulfides. Olivine commonly shows a pseudomorphic transformation to lizardite, and plagioclase grains generally are altered to fine aggregates of phyllosilicates. Where metamorphosed, the pyroxenes are partially replaced by amphiboles, olivine and specially the early-formed lizardite are replaced by antigorite, which develops interpenetrating plates that cut and overprint earlier pseudomorphic textures, and plagioclase is transformed into chlorite, epidote, calcite and minor scapolite. Minor talc, chlorite and secondary phlogopite also are present in the metamorphic assemblage.

The primary modal composition of these rocks is relatively constant along the ultramafic sequence except for a slight, irregular increase in the clinopyroxene: orthopyroxene ratio upward. Similarly, the composition of the major minerals exhibit a crude trend, with increasing Di in clinopyroxene and En in orthopyroxene, An in plagioclase, and Fo and especially Ni in olivine from

TABLE 1. WHOLE-ROCK COMPOSITIONS OF REPRESENTATIVE SAMPLES FROM DRILL CORES R695 AND R713, KEIVITSANSARVI Ni–Cu–PGE DEPOSIT

| Sample | SiO ₂ | TiO ₂ | Al ₂ O ₃ | Fe ₂ O ₃ | MnO | MgO | CaO | Na ₂ O | K ₂ O | P ₂ O ₅ | S | Cl | Cr | Ni | Cu | As | Total |
|------------------|------------------|------------------|--------------------------------|--------------------------------|------|-------|-------|-------------------|------------------|-------------------------------|------|------|------|------|------|------|-------|
| R695/80.00–80.50 | 45.71 | 0.34 | 6.32 | 7.82 | 0.10 | 18.48 | 14.18 | 0.66 | 0.23 | 0.01 | 1.05 | 0.17 | 0.17 | 1.07 | 0.18 | 0.00 | 96.49 |
| R695/81.00–81.50 | 46.23 | 0.40 | 5.43 | 7.44 | 0.11 | 17.66 | 15.84 | 0.68 | 0.29 | 0.01 | 0.87 | 0.28 | 0.19 | 0.85 | 0.17 | 0.00 | 96.51 |
| R695/84.00–84.50 | 47.60 | 0.41 | 3.67 | 7.75 | 0.11 | 18.60 | 15.98 | 0.54 | 0.11 | 0.01 | 1.02 | 0.13 | 0.20 | 1.02 | 0.17 | 0.00 | 97.32 |
| R695/84.50–85.00 | 47.44 | 0.43 | 2.97 | 7.95 | 0.11 | 19.14 | 16.03 | 0.49 | 0.11 | 0.01 | 1.03 | 0.18 | 0.21 | 1.02 | 0.17 | 0.00 | 97.29 |
| R695/85.50–86.00 | 47.77 | 0.37 | 4.78 | 6.78 | 0.11 | 19.31 | 16.06 | 0.66 | 0.18 | 0.00 | 0.45 | 0.27 | 0.22 | 0.49 | 0.08 | 0.00 | 97.53 |
| R713/19.00–19.50 | 48.40 | 0.38 | 2.30 | 7.90 | 0.09 | 21.89 | 14.54 | 0.20 | 0.05 | 0.00 | 0.28 | 0.09 | 0.22 | 0.46 | 0.01 | 0.00 | 96.81 |
| R713/22.00–22.50 | 48.69 | 0.38 | 2.21 | 8.06 | 0.09 | 21.39 | 13.68 | 0.14 | 0.06 | 0.00 | 0.29 | 0.03 | 0.17 | 0.41 | 0.00 | 0.00 | 95.60 |
| R713/23.00–23.50 | 47.40 | 0.38 | 2.26 | 9.84 | 0.08 | 21.14 | 13.55 | 0.12 | 0.03 | 0.00 | 0.88 | 0.04 | 0.18 | 1.09 | 0.01 | 0.00 | 97.00 |
| R713/29.00–29.50 | 45.99 | 0.37 | 3.94 | 8.03 | 0.11 | 18.88 | 13.77 | 0.22 | 0.58 | 0.01 | 0.56 | 0.07 | 0.16 | 0.65 | 0.01 | 0.03 | 93.38 |
| R713/29.50–30.00 | 47.82 | 0.46 | 3.26 | 7.78 | 0.13 | 17.34 | 16.05 | 0.33 | 0.57 | 0.01 | 0.34 | 0.10 | 0.15 | 0.42 | 0.01 | 0.05 | 94.82 |
| R713/39.00–39.50 | 45.96 | 0.33 | 5.19 | 7.53 | 0.09 | 18.76 | 15.35 | 0.65 | 0.10 | 0.00 | 1.32 | 0.14 | 0.20 | 1.43 | 0.24 | 0.00 | 97.29 |
| R713/40.50–41.00 | 43.96 | 0.32 | 4.72 | 8.08 | 0.12 | 18.45 | 15.49 | 0.28 | 0.14 | 0.00 | 1.55 | 0.14 | 0.18 | 1.61 | 0.05 | 0.01 | 95.10 |

Compositions are quoted in wt. %

the lower ores upward. Representative whole-rock compositions of selected samples from the drill cores studied are listed in Table 1.

These mineralogical and chemical variations occur along with an increasing abundance of komatiite xenoliths (in some cases containing pelitic intercalations) in the host ultramafic rocks toward the top of the ore deposit. Toward the roof of the intrusion, the abundance and size of the xenoliths increase; these vary from mm-size single crystals of olivine to bodies one hundred meters across (Mutanen 1997). These arguments, together with other trace-element (*e.g.*, REE) and isotope data (S, Sm–Nd and Re–Os; Huhma *et al.* 1996, Hanski *et al.* 1996), were used by Mutanen (1997) to develop a fractionation model based on the contamination of the parental melt of the Keivitsa–Satovaara Complex by the assimilation of pelites and black shales at the base of the magma chamber and by its chemical re-equilibration with komatiite xenoliths (plus small amounts of pelites) from the roof of the intrusion.

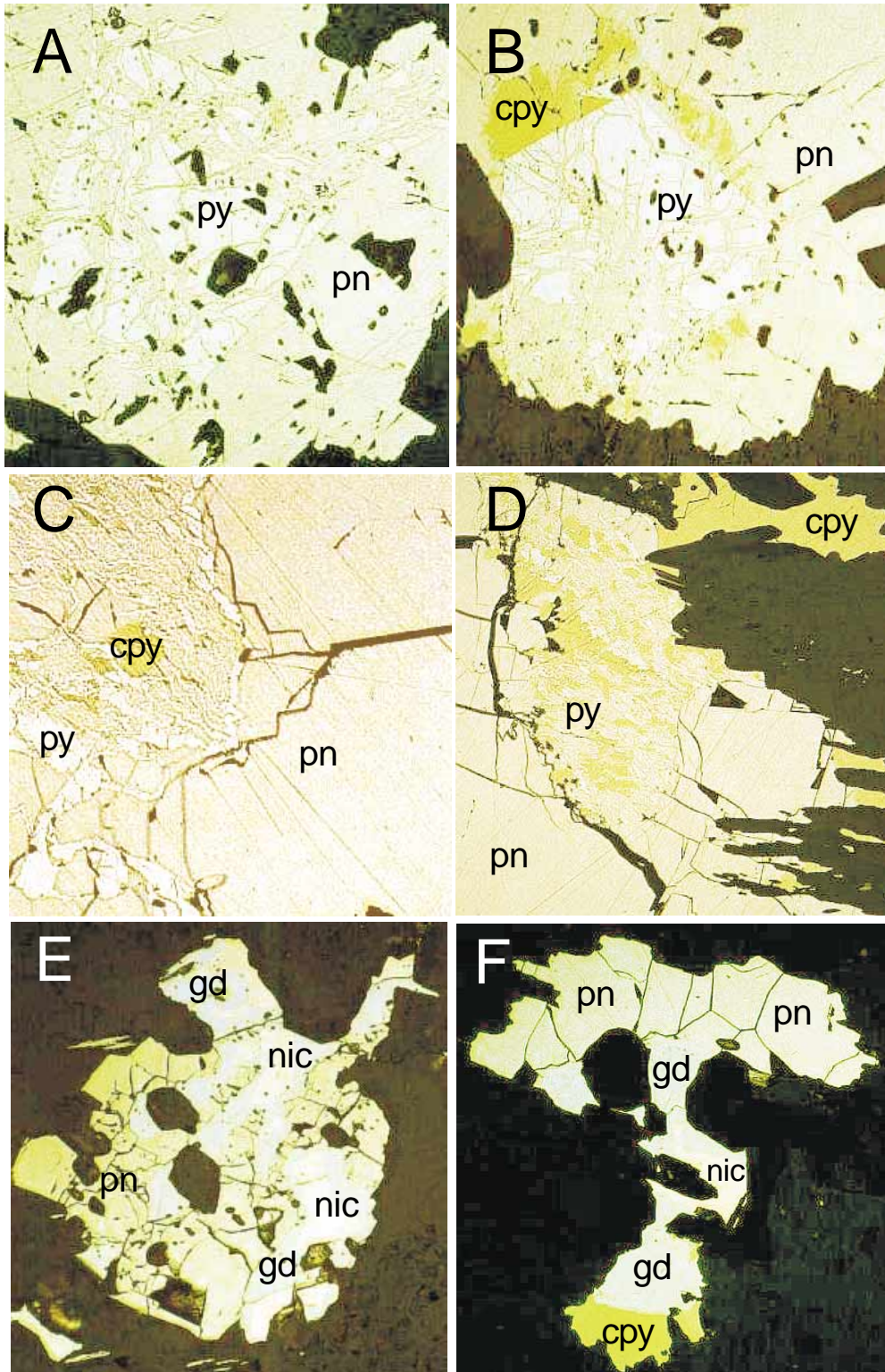
The sulfide ores

The Keivitsansarvi Ni–Cu–PGE deposit is a low-grade dissemination of sulfides, mainly characterized by significant variations in Ni content (from 87 ppm to ~5%) and in the Ni:Co ratio (from 1 to 80), associated with variations in the content of semimetals (As, Sb, Se, Te and Bi) and of noble metals (platinum-group elements and gold). From bottom to top, sulfide mineralization shows increasing amounts of Ni, semimetals and platinum-group elements.

In the samples of the upper section of the Keivitsansarvi deposit selected for this study, the sulfides are invariably interstitial to silicates, unless they were remobilized by late metamorphic fluids. In the latter case, sulfides (and arsenides) occur close to their primary lo-

cation, filling fractures, included in, and following the cleavage planes of amphiboles, chlorite and antigorite, and exhibiting irregular, serrated contacts with these metamorphic silicates. They also develop a fine dusting (submicrometric scale) throughout the serpentinized olivine (replaced by lizardite). The mineral assemblage varies slightly from one drill core to the next. In the samples from drill core R695, the main sulfides are pentlandite, pyrite and chalcopyrite; monoclinic pyrrhotite and millerite occur occasionally, and gersdorffite, bornite and mackinawite are rare. Pyrite displays textural patterns varying from variably fractured, euhedral to subhedral crystals included in pentlandite or chalcopyrite to extremely fine intergrowths with pentlandite and, to a lesser extent, chalcopyrite (Figs. 2A–D). It is possible to observe all intermediate stages between

FIG. 2. Reflected-light microscopy images of sulfide, arsenide and sulfarsenide intergrowth textures from the upper section of Keivitsansarvi deposit. A. Broken and partly dissolved pyrite (py) in pentlandite (pn) matrix, sample R713/22.40 m, width of the image 250 μ m. B. Pyrite intergrown with pentlandite and chalcopyrite (cpy) within pentlandite, sample R713/22.40 m, width of the image 550 μ m. C. Graphic intergrowth consisting of thin bands of pyrite and chalcopyrite within pentlandite, sample R695/81.15 m, width of the image 125 μ m. D. Graphic intergrowth of pyrite and chalcopyrite at the margins of a pentlandite crystal, sample R695/81.15 m, width of the image 250 μ m. E. Aggregate of pentlandite, and gersdorffite (gd) surrounding niccolite (nic), sample R713/29.95 m, width of the image 250 μ m. F. Interstitial pentlandite and chalcopyrite with niccolite and gersdorffite, sample R713/29.97 m, width of the image 250 μ m.



the textural relationships described; in these cases, pyrite seems to be replaced by pentlandite and chalcopyrite. Fine intergrowths of pentlandite and chalcopyrite occur occasionally along the contact between these two minerals. Chalcopyrite also occur filling late fractures in silicates. Monoclinic pyrrhotite is associated with chalcopyrite, pyrite, and granular pentlandite, and usually exhibits abundant flame-shaped exsolution-induced blebs of pentlandite. Millerite is associated with pentlandite and is the main constituent of the dusting of sulfides in the pseudomorphic lizardite. Gersdorffite forms euhedral to subhedral crystals included in pentlandite and chalcopyrite. Mackinawite replaces pentlandite, and bornite invariably occurs in association with chalcopyrite. The samples from drill core R713 show almost the same mineralogy and texture as those from R695, although they are rich in nickeline, maucherite and, especially, gersdorffite (Figs. 2E–F). Nickeline and maucherite occur separately but are associated with chalcopyrite and pentlandite (or pentlandite–pyrite intergrowths), or both, and are invariably surrounded by gersdorffite. The latter is locally replaced along outer grain-boundaries by a second generation of maucherite and, in rare cases, it exhibits minute inclusions of pyrrhotite and pentlandite at the replacement front. Gersdorffite also forms isolated euhedral to subhedral crystals included in or, more commonly, at the grain boundaries of pentlandite.

Electron-microprobe analyses of the main sulfides show that Ni content of pentlandite is very variable, from 33 to 42 wt.% Ni (26–32.5 at.%); Ni:Fe ratios fall between 1.0 and 1.55 (Table 2). This chemical variability is closely related to the mineral assemblage. In the pentlandite–pyrite assemblage (containing small amounts of chalcopyrite), the Ni content of pentlandite varies from 30 to 32.5 at.%, whereas in the assemblage pentlandite – pyrite – monoclinic pyrrhotite – chalcopyrite, pentlandite contains between 26 and 27 at.% Ni. These compositional ranges indicate that the pentlandite from the upper section of the Keivitsansarvi deposit is similar to that equilibrated at relatively low temperature in association with pyrite, pyrrhotite or millerite in the Marbridge deposit, Quebec (Graterol & Naldrett 1971). In fact, the composition reported here for pentlandite in the pentlandite–pyrite assemblage overlaps that of pentlandite in the divariant field of pentlandite–pyrite in the condensed system Fe–Ni–S at 230°C (Misra & Fleet 1973). The coexisting pyrite contains 0.17–1.97 at.% Ni and 0.18–2.37 at.% Co, and the pyrrhotite contains 0.09–0.77 at.% Ni (Table 2). The Ni and Co contents of pyrite are higher than those of pyrite associated with pentlandite, pyrrhotite and millerite in the Marbridge deposit (Graterol & Naldrett 1971) and, according to the results of Misra & Fleet (1973), could be explained by assuming temperatures of equilibration above 140°C for the assemblage pentlandite – pyrite – chalcopyrite – monoclinic pyrrhotite described here. The composition of the pyrrhotite suggests that Ni dif-

fusion stopped at very low temperatures, in agreement with phase relations at 140°C (Misra & Fleet 1973).

The composition of gersdorffite also indicates that its final re-equilibration took place at a relatively low temperature. This mineral shows a wide compositional range, from $(\text{Ni}_{0.54}\text{Co}_{0.35}\text{Fe}_{0.10})_{\Sigma 0.99}\text{As}_{0.99}\text{S}_{1.0}$ to the Co- and Fe-free Ni end-member, with a Co:Fe ratio varying from 0.33 to 3.69, and with nearly constant metal to non-metal ratio. From Klemm's (1965) experimental results in the system NiAsS–CoAsS–FeAsS, these compositions correspond to gersdorffite grains crystallized or re-equilibrated on cooling below 500°C. The analyzed nickeline and maucherite contain minor amounts of Fe (0.28–0.87 and 0.1–1.67 at.%, respectively) and less than 0.1 at.% Co.

THE PLATINUM-GROUP MINERALS

A total of 120 grains of platinum-group minerals (PGM) were found in fifteen selected polished sections from the two drill cores studied. Of these grains, 54% occur as isolated PGM grains included in silicates (cumulus pyroxenes in some cases, but mainly hydrous silicates: amphibole, antigorite and chlorite), 39% are associated with sulfides (attached to grain boundaries),

TABLE 2. REPRESENTATIVE RESULTS OF ELECTRON-MICROPROBE ANALYSES OF SULFIDES AND SULFARSENIDES FROM DRILL CORES R695 AND R713, KEIVITSANSARVI Ni–Cu–PGE DEPOSIT

| Anal./Min. | | Ni | Co | Fe | Cu | As | Sb | Se | S | Total |
|------------|----|----------------------------------|-------|-------|-------|-------|------|------|-------|---------------|
| 1 | Pn | 41.43 | 0.32 | 25.74 | n.a. | 0.06 | 0.00 | n.a. | 32.18 | 99.73 |
| 2 | Pn | 38.75 | 0.45 | 27.97 | n.a. | 0.00 | 0.03 | n.a. | 31.81 | 99.01 |
| 3 | Pn | 33.40 | 0.32 | 31.70 | 0.00 | 0.00 | 0.00 | 0.09 | 33.51 | 99.02 |
| 4 | Py | 2.89 | 0.81 | 43.97 | 0.03 | 0.05 | 0.01 | 0.08 | 52.77 | 100.61 |
| 5 | Py | 0.72 | 3.49 | 41.85 | 0.34 | 0.04 | 0.01 | 0.11 | 53.63 | 100.19 |
| 6 | Py | 0.29 | 2.43 | 43.72 | 0.00 | 0.00 | 0.00 | 0.08 | 53.60 | 100.12 |
| 7 | Po | 1.04 | 0.00 | 58.39 | 0.01 | 0.00 | 0.00 | 0.08 | 39.65 | 99.17 |
| 8 | Cp | 0.00 | 0.00 | 30.30 | 34.05 | 0.02 | 0.00 | 0.05 | 35.09 | 99.51 |
| 9 | Gd | 18.74 | 12.44 | 3.40 | 0.00 | 44.74 | 0.02 | 0.31 | 19.45 | 99.10 |
| 10 | Gd | 29.96 | 4.38 | 1.48 | n.a. | 45.39 | 0.14 | n.a. | 19.30 | 100.65 |
| 11 | Gd | 35.30 | 0.10 | 0.28 | n.a. | 45.49 | 0.05 | n.a. | 19.13 | 100.35 |
| | | Formula proportions ^a | | | | | | | | <i>Me/nMe</i> |
| 1 | Pn | 5.51 | 0.04 | 3.60 | n.a. | 0.01 | 0.00 | n.a. | 7.84 | 1.17 |
| 2 | Pn | 5.19 | 0.06 | 3.94 | n.a. | 0.00 | 0.00 | n.a. | 7.80 | 1.18 |
| 3 | Pn | 4.42 | 0.04 | 4.41 | 0.00 | 0.00 | 0.00 | 0.01 | 8.12 | 1.09 |
| 4 | Py | 0.06 | 0.02 | 0.95 | 0.00 | 0.00 | 0.00 | 0.00 | 1.98 | 0.52 |
| 5 | Py | 0.01 | 0.07 | 0.90 | 0.01 | 0.00 | 0.00 | 0.00 | 2.01 | 0.49 |
| 6 | Py | 0.01 | 0.05 | 0.94 | 0.00 | 0.00 | 0.00 | 0.00 | 2.00 | 0.50 |
| 7 | Po | 0.01 | 0.00 | 0.84 | 0.00 | 0.00 | 0.00 | 0.00 | 1.00 | 0.86 |
| 8 | Cp | 0.00 | 0.00 | 1.00 | 0.99 | 0.00 | 0.00 | 0.00 | 2.01 | 0.99 |
| 9 | Gd | 0.53 | 0.35 | 0.10 | 0.00 | 1.00 | 0.00 | 0.01 | 1.01 | 0.49 |
| 10 | Gd | 0.84 | 0.12 | 0.04 | n.a. | 1.00 | 0.00 | n.a. | 0.99 | 0.51 |
| 11 | Gd | 1.00 | 0.00 | 0.01 | n.a. | 1.01 | 0.00 | n.a. | 0.99 | 0.50 |

Anal.: analysis number. Min.: Mineral. Symbols: Pn: pentlandite, Py: pyrite, Po: pyrrhotite, Cp: chalcopyrite, Gd: gersdorffite. n.a.: not analyzed. *Me/nMe*: metal to non-metal ratio. # Based on a total of seventeen (pentlandite), three (pyrite and gersdorffite) and four (chalcopyrite) atoms per formula unit (*apfu*). The formula of pyrrhotite is based on S + Se + As + Sb = 1 *apfu*. Compositions are quoted in wt.% and *apfu*.

and only 6% of the grains occur included in sulfides. Their grain size is very small, ranging from a sub-roundish crystal of 35 μm across to grains less than 1 μm . Most of the identified PGM (80%) correspond to

TABLE 3. REPRESENTATIVE RESULTS OF ELECTRON-MICROPROBE ANALYSES OF MONCHEITE FROM DRILL CORES R695 AND R713, KEIVITSANSARVI Ni–Cu–PGE DEPOSIT

| Anal. | Pt | Pd | Rh | Os | Ir | Ni | Fe | Cu | Te | Bi | Sb | Total |
|-------|-------|-------|------|------|------|------|------|------|-------|-------|------|--------|
| 1 | 39.25 | 0.21 | 0.04 | 0.17 | 0.05 | 0.20 | 0.17 | 0.00 | 42.51 | 18.81 | n.a. | 101.41 |
| 2 | 40.78 | 0.00 | 0.07 | 0.16 | 0.00 | 0.10 | 0.14 | 0.00 | 42.50 | 17.81 | n.a. | 101.56 |
| 3 | 35.04 | 3.58 | 0.18 | 0.24 | 0.14 | 0.18 | 0.55 | 0.31 | 42.87 | 17.72 | n.a. | 100.81 |
| 4 | 30.49 | 5.26 | 0.06 | 0.00 | 0.11 | 0.28 | 0.77 | 0.24 | 48.19 | 14.12 | n.a. | 99.52 |
| 5 | 19.64 | 10.48 | 0.00 | 0.38 | 0.18 | 1.83 | 0.56 | 0.05 | 49.89 | 17.14 | 0.36 | 100.51 |
| 6 | 31.26 | 3.90 | 0.21 | 0.40 | 0.00 | 0.07 | 0.13 | 0.02 | 40.84 | 22.27 | 0.31 | 99.41 |
| 7 | 25.83 | 8.20 | 0.00 | 0.37 | 0.01 | 0.52 | 0.06 | 0.07 | 42.73 | 22.50 | 0.54 | 100.83 |
| 8 | 22.10 | 10.69 | 0.08 | 0.39 | 0.18 | 1.38 | 0.45 | 0.15 | 49.93 | 16.03 | 0.24 | 101.62 |
| 9 | 32.44 | 5.05 | 0.00 | 0.31 | 0.00 | 0.35 | 0.35 | 0.07 | 51.77 | 10.71 | 0.31 | 101.36 |
| 10 | 37.81 | 0.61 | 0.01 | 0.47 | 0.09 | 0.00 | 0.28 | 0.00 | 44.44 | 15.09 | 0.30 | 99.10 |

| Formula proportions ^a | | | | | | | | | | | | Me/Me |
|----------------------------------|------|------|------|------|------|------|------|------|------|------|------|-------|
| Pt | Pd | Rh | Os | Ir | Ni | Fe | Cu | Te | Bi | Sb | | |
| 1 | 0.95 | 0.01 | 0.00 | 0.00 | 0.00 | 0.02 | 0.01 | 0.00 | 1.57 | 0.43 | n.a. | 0.50 |
| 2 | 0.99 | 0.00 | 0.00 | 0.00 | 0.00 | 0.01 | 0.01 | 0.00 | 1.57 | 0.40 | n.a. | 0.51 |
| 3 | 0.82 | 0.15 | 0.01 | 0.01 | 0.00 | 0.01 | 0.04 | 0.02 | 1.54 | 0.39 | n.a. | 0.55 |
| 4 | 0.69 | 0.22 | 0.00 | 0.00 | 0.00 | 0.02 | 0.06 | 0.02 | 1.67 | 0.30 | n.a. | 0.51 |
| 5 | 0.42 | 0.41 | 0.00 | 0.01 | 0.00 | 0.13 | 0.04 | 0.00 | 1.62 | 0.34 | 0.01 | 0.51 |
| 6 | 0.76 | 0.17 | 0.01 | 0.01 | 0.00 | 0.01 | 0.01 | 0.00 | 1.51 | 0.50 | 0.01 | 0.48 |
| 7 | 0.59 | 0.35 | 0.00 | 0.01 | 0.00 | 0.04 | 0.00 | 0.00 | 1.50 | 0.48 | 0.02 | 0.50 |
| 8 | 0.47 | 0.42 | 0.00 | 0.01 | 0.00 | 0.10 | 0.03 | 0.01 | 1.62 | 0.32 | 0.01 | 0.53 |
| 9 | 0.72 | 0.21 | 0.00 | 0.01 | 0.00 | 0.03 | 0.03 | 0.00 | 1.77 | 0.22 | 0.01 | 0.50 |
| 10 | 0.92 | 0.03 | 0.00 | 0.01 | 0.00 | 0.00 | 0.02 | 0.00 | 1.66 | 0.34 | 0.01 | 0.49 |

Anal.: Analysis number. n.a.: not analyzed. Me/Me: Metal to semimetal ratio.
^a Based on a total of three atoms in the formula unit. Compositions are quoted in wt.% and *appfu*.

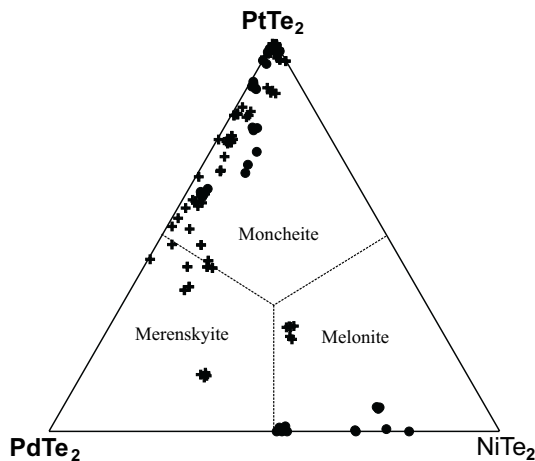


FIG. 3. Molar proportions of moncheite, merenskyite and melonite from upper part of the Keivitsansarvi deposit plotted in the PtTe_2 – PdTe_2 – NiTe_2 diagram. Symbols: dots, samples from drill core R–695; crosses, samples from drill core R–713.

minerals in the system Pt–Pd–Ni–Te–Bi, including moncheite, merenskyite, michenerite, Pt- and Pd-rich melonite, and minerals of the kotulskite – sobolevskite – (sudburyite) solid-solution series. Sperrylite grains are abundant as well, representing 14% of the total PGM found. Other PGM encountered are cooperite, braggite, Pt–Fe alloys and mertieite II or stibiopalladinite. Some grains of native gold also were found.

PGM of the system Pt–Pd–Ni–Te–Bi

Moncheite [(Pt, Pd, Ni) (Te, Bi)₂] is the most abundant mineral of this group, representing 55% of the telluride–bismuthide grains found. It occurs as relatively large grains (from 35 to 5 μm) included in silicates, at silicate–sulfide grain boundaries or, less commonly, at pentlandite–millerite grain boundaries or associated with chalcopyrite filling late fractures in silicates. Its chemical composition shows an extensive substitution of Te for Bi and of Pt for Pd (Table 3, Figs. 3, 4). Bi content varies from 7.16 to 22.24 at.%, and Pd substitution for Pt extends from the composition of Pd-free moncheite to that of platinum merenskyite (Figs. 3, 4), in agreement with the existence of complete solid-solution between merenskyite and moncheite. Minor amounts of Ni (<4.95 at.%), Fe (<4.29 at.%), As (<1.19 at.%) and Sb (<1.05 at.%) also are present. The chemi-

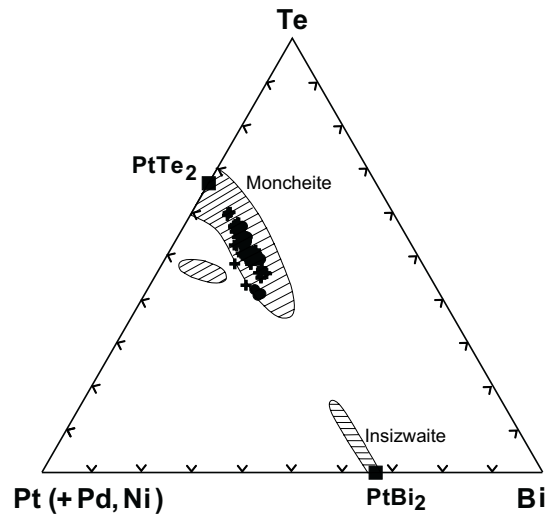


FIG. 4. Pt(+Pd, Ni)–Te–Bi diagram showing the compositional variation (in at.%) of moncheite from the upper part of the Keivitsansarvi deposit. The fields of the reported composition of moncheite and insizwaite [taken from Harney & Merkle (1990)] are drawn for comparison. Symbols: dots: samples from drill core R–695; crosses: samples from drill core R–713, and squares: stoichiometric composition of moncheite and insizwaite.

cal composition of the moncheite plots within the compositional range reported in the literature (Fig. 4).

Merenskyite [(Pd, Pt, Ni) (Te, Bi)₂] and *melonite* [(Ni, Pd, Pt) (Te, Bi)₂] are less abundant (13% and 9% of the total telluride–bismuthide grains, respectively), and the grains are smaller (<10 μm) than in the case of moncheite. They mainly occur associated with sulfides as inclusions in silicates or attached to grain boundaries of pyrite, pentlandite, millerite or chalcopyrite between the silicates. Pt-, Ni- and Bi-free merenskyite has not been found; on the contrary, most analyzed grains correspond to platinumian merenskyite containing important

amounts of Bi (up to 11.69 at.%; Table 4, Figs. 3, 5). Only one grain shows a chemical composition departing from this tendency: (Pd_{0.58}Ni_{0.26}Pt_{0.14}Fe_{0.05})Σ1.03 (Te_{1.63}Bi_{0.31}As_{0.02})Σ1.96 (anal. 1 in Table 4). The chemical composition of the few grains of melonite found plots

TABLE 4. REPRESENTATIVE RESULTS OF ELECTRON-MICROPROBE ANALYSES OF MERENSKYITE, MELONITE AND MICHENERITE FROM DRILL CORES R695 AND R713, KEIVITSANSARVI Ni–Cu–PGE DEPOSIT

| Anal. | Pt | Pd | Os | Ni | Fe | Cu | Te | Bi | Sb | As | Total |
|-------|-------|-------|------|-------|------|------|-------|-------|------|------|--------|
| 1 | 7.31 | 16.18 | 0.00 | 4.00 | 0.70 | 0.00 | 54.75 | 16.78 | n.a. | 0.32 | 100.04 |
| 2 | 19.37 | 11.01 | 0.42 | 1.95 | 0.56 | 0.01 | 50.38 | 16.10 | 0.28 | 0.05 | 100.13 |
| 3 | 18.95 | 10.58 | 0.33 | 2.10 | 0.63 | 0.04 | 49.58 | 17.62 | 0.27 | 0.01 | 100.11 |
| 4 | 10.81 | 8.57 | 0.00 | 5.82 | 0.58 | 0.22 | 49.60 | 22.92 | n.a. | 0.00 | 98.52 |
| 5 | 3.37 | 7.04 | 0.00 | 11.61 | 0.60 | 0.00 | 72.42 | 3.18 | 0.69 | 0.00 | 98.91 |
| 6 | 3.13 | 7.09 | 0.00 | 11.44 | 0.56 | 0.07 | 73.27 | 3.02 | 0.55 | 0.00 | 99.13 |
| 7 | 0.85 | 24.51 | 0.22 | 0.02 | 0.68 | 0.00 | 30.72 | 44.39 | 1.20 | 0.28 | 102.87 |

| | Formula proportions [#] | | | | | | | | | | <i>Me/nMe</i> |
|---|----------------------------------|------|------|------|------|------|------|------|------|------|---------------|
| 1 | 0.14 | 0.58 | 0.00 | 0.26 | 0.05 | 0.00 | 1.63 | 0.31 | n.a. | 0.02 | 0.53 |
| 2 | 0.41 | 0.43 | 0.01 | 0.14 | 0.04 | 0.00 | 1.63 | 0.32 | 0.01 | 0.00 | 0.53 |
| 3 | 0.40 | 0.41 | 0.01 | 0.15 | 0.05 | 0.00 | 1.62 | 0.35 | 0.01 | 0.00 | 0.52 |
| 4 | 0.22 | 0.32 | 0.00 | 0.39 | 0.04 | 0.01 | 1.54 | 0.43 | n.a. | 0.00 | 0.50 |
| 5 | 0.06 | 0.23 | 0.00 | 0.67 | 0.04 | 0.00 | 1.93 | 0.05 | 0.02 | 0.00 | 0.50 |
| 6 | 0.05 | 0.23 | 0.00 | 0.66 | 0.03 | 0.00 | 1.95 | 0.05 | 0.02 | 0.00 | 0.48 |
| 7 | 0.02 | 0.97 | 0.01 | 0.00 | 0.05 | 0.00 | 1.01 | 0.89 | 0.04 | 0.02 | 0.54 |

Anal.: Analysis number. 1–3: merenskyite, 4–6: melonite, and 7: michenerite. n.a.: not analyzed. *Me/nMe*: Metal to non metal ratio. # Based on a total of three atoms in the formula unit. Compositions are quoted in wt.% and *appfu*.

TABLE 5. REPRESENTATIVE RESULTS OF ELECTRON-MICROPROBE ANALYSES OF MINERALS OF THE KOTULSKITE – SOBOLEVSKITE – (SUDBURYITE) SOLID-SOLUTION SERIES FROM DRILL CORES R695 AND R713, KEIVITSANSARVI Ni–Cu–PGE DEPOSIT

| Anal. | Pt | Pd | Ru | Os | Ir | Ni | Fe | Cu | Te | Bi | Sb | As | Total |
|-------|------|-------|------|------|------|------|------|------|-------|-------|-------|------|--------|
| 1 wt% | 0.00 | 39.64 | 0.00 | 0.16 | 0.08 | 0.15 | 0.49 | 0.20 | 40.82 | 18.01 | 0.41 | 0.00 | 99.96 |
| 2 | 0.00 | 38.08 | 0.10 | 0.21 | 0.00 | 0.13 | 0.73 | 0.14 | 24.74 | 29.99 | 5.30 | 0.00 | 99.42 |
| 3 | 0.48 | 36.60 | 0.01 | 0.39 | 0.08 | 0.08 | 0.35 | 0.00 | 6.70 | 44.05 | 11.27 | 0.38 | 100.39 |
| 4 | 0.49 | 31.29 | 0.14 | 0.45 | 0.21 | 0.04 | 1.10 | 0.18 | 1.07 | 60.61 | 6.11 | 1.03 | 102.72 |
| 5 | 0.69 | 36.71 | 0.09 | 0.33 | 0.04 | 0.17 | 0.96 | 0.08 | 9.37 | 44.08 | 8.77 | 0.00 | 101.29 |

| | Formula proportions [#] | | | | | | | | | | | | <i>Me/nMe</i> |
|----------------|----------------------------------|------|------|------|------|------|------|------|------|------|------|------|---------------|
| 1 <i>appfu</i> | 0.00 | 0.93 | 0.00 | 0.00 | 0.00 | 0.01 | 0.02 | 0.01 | 0.80 | 0.22 | 0.01 | 0.00 | 0.94 |
| 2 | 0.00 | 0.94 | 0.00 | 0.00 | 0.00 | 0.01 | 0.03 | 0.01 | 0.51 | 0.38 | 0.11 | 0.00 | 0.99 |
| 3 | 0.01 | 0.96 | 0.00 | 0.01 | 0.00 | 0.00 | 0.02 | 0.00 | 0.15 | 0.59 | 0.26 | 0.01 | 0.99 |
| 4 | 0.01 | 0.85 | 0.00 | 0.01 | 0.00 | 0.00 | 0.06 | 0.01 | 0.02 | 0.84 | 0.15 | 0.04 | 0.90 |
| 5 | 0.01 | 0.95 | 0.00 | 0.00 | 0.00 | 0.01 | 0.05 | 0.00 | 0.20 | 0.58 | 0.20 | 0.00 | 1.04 |

Anal.: Analysis number. *Me/nMe*: Metal to non metal ratio. # Based on a total of two atoms in the formula unit.

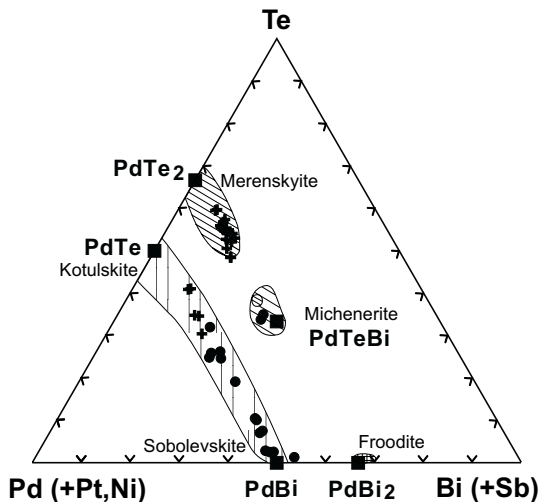


FIG. 5. Pd(+Pt, Ni)–Te–(Bi+Sb) diagram showing the compositional variation in at.% of merenskyite, kotulskite – sobolevskite solid solution and michenerite in the upper part of the Keivitsansarvi deposit. The fields of the reported composition of merenskyite, michenerite and froodite [taken from Harney & Merkle (1990)] as well as that of the kotulskite–sobolevskite solid-solution series [taken from Evstigneeva *et al.* (1976) and Harney & Merkle (1990)] are drawn for comparison. Symbols: dots: samples from drill core R–695, crosses: samples from drill core R–713, squares: stoichiometric composition of merenskyite, kotulskite, michenerite, sobolevskite and froodite.

in three different small regions of the melonite compositional field within the system $\text{NiTe}_2\text{-PdTe}_2\text{-PtTe}_2$ (Fig. 3, Table 5), corresponding to the formulae: $(\text{Ni}_{0.67}\text{Pd}_{0.23}\text{Pt}_{0.06}\text{Fe}_{0.04})_{\Sigma 1.0}(\text{Te}_{1.93}\text{Bi}_{0.05}\text{Sb}_{0.02})_{\Sigma 2.0}$, $(\text{Ni}_{0.39}\text{Pd}_{0.32}\text{Pt}_{0.22}\text{Fe}_{0.04}\text{Cu}_{0.01})_{\Sigma 0.98}(\text{Te}_{1.54}\text{Bi}_{0.43})_{\Sigma 1.97}$ and $(\text{Ni}_{0.48}\text{Pd}_{0.46}\text{Fe}_{0.07}\text{Pt}_{0.01})_{\Sigma 1.02}(\text{Te}_{1.73}\text{Bi}_{0.21}\text{Sb}_{0.02}\text{As}_{0.02}\text{S}_{0.01})_{\Sigma 1.99}$.

Only four grains of *michenerite* (PdBiTe) have been found. Two of them occur within hydrous silicate, and the two others are associated with chalcopyrite, filling a narrow fracture in hydrous silicate. Their grain size varies from $9 \times 5 \mu\text{m}$ to $2 \times 1 \mu\text{m}$; they present irregular, curved grain-boundaries. Electron-microprobe analysis of the largest grain gives a Ni-free, metal-rich composition, corresponding to the formula: $(\text{Pd}_{0.97}\text{Fe}_{0.05}\text{Pt}_{0.02}\text{Os}_{0.01})_{\Sigma 1.05}(\text{Bi}_{0.89}\text{Sb}_{0.04}\text{As}_{0.02})_{\Sigma 0.95}\text{Te}_{1.01}$.

Minerals of the *kotulskite - sobolevskite - (sudburyite)* solid-solution series occur as elongate, small irregular grains (the largest measures $12 \times 7 \mu\text{m}$) included in hydrous silicates or at silicate-sulfide grain boundaries. They commonly are fractured and cut by late laths of chlorite or antigorite. As shown in Figures 5 and 6 and Table 5, the analyzed grains extend in composition from bismuthian kotulskite $[(\text{Pd}_{0.93}\text{Fe}_{0.02})_{\Sigma 0.95}(\text{Te}_{0.81}\text{Bi}_{0.21}\text{Sb}_{0.01})_{\Sigma 1.03}]$ to antimonial sobolevskite $[(\text{Pd}_{0.97}\text{Fe}_{0.03}\text{Ni}_{0.01}\text{Pt}_{0.01}\text{Os}_{0.01})_{\Sigma 1.03}(\text{Bi}_{0.62}\text{Sb}_{0.29}\text{Te}_{0.05}\text{S}_{0.01})_{\Sigma 0.97}]$. This compositional trend provides further evidence of the existence of continuous solid-solution between kotulskite and sobolevskite, as shown by Evstigneeva *et al.* (1976), but with a substitution of Te for Bi + Sb, confirming their assumption of the prob-

able existence of phases intermediate among kotulskite, sobolevskite and sudburyite. Pd substitution for Pt and Ni is negligible (Table 5).

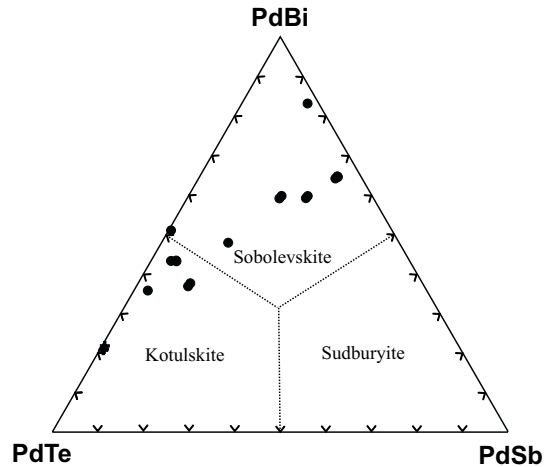


FIG. 6. Composition of kotulskite - sobolevskite - (sudburyite) solid-solution series in at.% from the upper part of the Keivitsansarvi deposit plotted in the PdBi-PdTe-PdSb diagram. Symbols: dots: samples from drill core R-695, and crosses: samples from drill core R-713.

TABLE 6. REPRESENTATIVE RESULTS OF ELECTRON-MICROPROBE ANALYSES OF SPERRYLITE, COOPERITE AND BRAGGITE FROM DRILL CORES R695 AND R713, KEIVITSANSARVI Ni-Cu-PGE DEPOSIT

| Anal. | Pt | Pd | Rh | Os | Ir | Au | Ni | Fe | Cu | As | Bi | Sb | S | Total | |
|----------------------------------|-------|------|------|------|------|------|------|------|------|-------|-------|------|-------|--------|--------|
| 1 wt% | 53.99 | 0.00 | 0.19 | 0.11 | 0.17 | 0.00 | 0.00 | 0.96 | 0.76 | 0.00 | 42.03 | 0.08 | 1.61 | 0.04 | 99.94 |
| 2 | 54.26 | 0.00 | 0.30 | 0.22 | 0.01 | 0.00 | 0.00 | 1.15 | 0.90 | 0.00 | 42.42 | 0.27 | 1.24 | 0.00 | 100.77 |
| 3 | 54.01 | 0.07 | 0.37 | 0.36 | 0.18 | 0.00 | 0.89 | 1.24 | 0.00 | 0.00 | 40.85 | 0.00 | 0.93 | 0.13 | 99.03 |
| 4 | 53.01 | 0.00 | 0.08 | 0.34 | 0.06 | 0.14 | 1.13 | 0.96 | 0.00 | 0.00 | 41.67 | 0.06 | 1.95 | 0.21 | 99.61 |
| 5 | 52.38 | 0.00 | 0.34 | 0.35 | 3.35 | 0.00 | 0.21 | 0.38 | 0.00 | 0.00 | 42.30 | 0.02 | 0.77 | 0.69 | 100.79 |
| 6 | 54.00 | 0.07 | 0.40 | 0.32 | 0.11 | 0.52 | 0.23 | 0.38 | 0.14 | 41.60 | 0.00 | 2.58 | 0.18 | 100.53 | |
| 7 | 77.83 | 1.98 | 0.33 | 0.56 | 0.16 | 0.51 | 1.16 | 1.38 | 0.33 | 0.30 | 0.13 | n.a. | 14.17 | 98.84 | |
| 8 | 69.14 | 5.12 | 0.30 | 0.42 | 0.04 | 0.00 | 7.07 | 1.13 | 0.00 | 0.00 | 0.02 | n.a. | 17.58 | 100.82 | |
| 9 | 67.99 | 3.91 | 0.41 | 0.44 | 0.00 | 0.00 | 6.74 | 1.49 | 0.01 | 0.52 | 0.12 | n.a. | 18.34 | 99.97 | |
| 10 | 68.87 | 3.82 | 0.24 | 0.35 | 0.08 | 0.00 | 6.50 | 1.20 | 0.11 | 0.17 | 0.00 | n.a. | 17.71 | 99.05 | |
| Formula proportions ^a | | | | | | | | | | | | | | | |
| 1 | 0.94 | 0.00 | 0.01 | 0.00 | 0.00 | 0.00 | 0.06 | 0.05 | 0.00 | 1.90 | 0.00 | 0.04 | 0.00 | 0.55 | |
| 2 | 0.93 | 0.00 | 0.01 | 0.00 | 0.00 | 0.00 | 0.07 | 0.05 | 0.00 | 1.90 | 0.00 | 0.03 | 0.00 | 0.55 | |
| 3 | 0.94 | 0.00 | 0.01 | 0.01 | 0.00 | 0.00 | 0.05 | 0.08 | 0.00 | 1.86 | 0.00 | 0.03 | 0.01 | 0.57 | |
| 4 | 0.91 | 0.00 | 0.00 | 0.01 | 0.00 | 0.00 | 0.06 | 0.06 | 0.00 | 1.87 | 0.00 | 0.05 | 0.02 | 0.54 | |
| 5 | 0.90 | 0.00 | 0.01 | 0.01 | 0.06 | 0.00 | 0.01 | 0.02 | 0.00 | 1.89 | 0.00 | 0.02 | 0.07 | 0.51 | |
| 6 | 0.94 | 0.00 | 0.01 | 0.01 | 0.00 | 0.01 | 0.01 | 0.02 | 0.01 | 1.89 | 0.00 | 0.07 | 0.02 | 0.51 | |
| 7 | 0.86 | 0.04 | 0.01 | 0.01 | 0.00 | 0.01 | 0.04 | 0.05 | 0.01 | 0.01 | 0.00 | n.a. | 0.96 | 1.06 | |
| 8 | 0.65 | 0.09 | 0.01 | 0.00 | 0.00 | 0.00 | 0.22 | 0.04 | 0.00 | 0.00 | 0.00 | n.a. | 1.00 | 1.01 | |
| 9 | 0.63 | 0.07 | 0.01 | 0.00 | 0.00 | 0.00 | 0.21 | 0.05 | 0.00 | 0.01 | 0.00 | n.a. | 1.03 | 0.93 | |
| 10 | 0.65 | 0.07 | 0.00 | 0.00 | 0.00 | 0.00 | 0.20 | 0.04 | 0.00 | 0.00 | 0.00 | n.a. | 1.02 | 0.94 | |

Anal: Analysis number. 1-6: sperrylite, 7: cooperite, and 8-10: braggite. n.a.: not analyzed. *Mel/nMe*: Ratio of metal to non metal atoms. # Based on a total of three (sperrylite) and two (cooperite and braggite) atoms in the formula unit.

Sperrylite (PtAs₂)

Sperrylite is, together with moncheite, the most abundant PGM in the upper section of the Keivitsansarvi Ni–Cu–PGE deposit. It occurs as rounded or irregular grains included in silicates, either isolated or associated with pentlandite. Only one grain was found included in pentlandite. Its grain size varies from 20 × 11 μm to 1 × 1.5 μm. Electron-microprobe analyses of the different grains (Table 6) reveal a composition with minor amounts of Fe (0.5–2.52 at.%), Ni (<2.18 at.%), Rh (0.09–0.65 at.%), Os (0.06–0.62 at.%) and Sb (<4.01 at.%). In addition, one isolated grain included in amphibole contains some Pd (1.28–1.72 at.%), and another grain, associated with pentlandite, contains significant amounts of Ir (1.65–2.13 at.%).

Cooperite (Pt,Pd)S and braggite (Pt,Pd,Ni)S

Two grains of Pt and Pd sulfides were identified during our study. Their grain sizes are 40 × 6 μm and 10 × 5 μm, respectively, and both occur at the contact between pentlandite and a hydrous silicate. The smaller grain contains 42.65–43.92 at.% Pt, 2.01–2.07 at.% Pd and 1.99–2.15 at.% Ni (anal. 7 in Table 6), which corresponds to cooperite with an average formula (Pt_{0.86}Fe_{0.05}

Pd_{0.04}Ni_{0.04}Cu_{0.01}Rh_{0.01}Os_{0.01})Σ1.02(S_{0.96}As_{0.01})Σ0.97. This formula shows high Fe content (2.56 at.% on average) considering that generally this element is not detected in cooperite (Verryn & Merkle 2000). Although this Fe content could be the result of a slight contamination owing to fluorescence from the associated hydrous silicate, it is lower than some values reported in the literature from the Merensky Reef (4.73 at.% Fe, Mostert *et al.* 1982), the Great Dyke (up to 5.87 at.% Fe, Coghill & Wilson 1993) and several placer deposits (2.85–4.33 at.% Fe, Cabri *et al.* 1996, Augé *et al.* 1998, Legendre & Augé 1992). In the larger grain, Pt, Pd and Ni contents vary, respectively, within the following ranges: 31.30–33.36 at.%, 2.74–4.60 at.% and 10.23–11.12 at.% (anal. 8, 9 and 10 in Table 6). Its average formula is (Pt_{0.64}Ni_{0.21}Pd_{0.07}Fe_{0.04}Rh_{0.01})Σ0.97S_{1.02}. Similar compositions encountered in the Stillwater complex have been attributed to low-Pt cooperite by Cabri *et al.* (1978) and Volborth *et al.* (1986). However, X-ray powder-diffraction data of Pt sulfides with nearly identical composition as those described here, from the Lulkulaisvaara layered intrusion, clearly indicate that these PGM belong to the braggite series (Barkov *et al.* 1995b). As in the cooperite described, the Fe content of braggite exceeds most of the values reported in the literature (*e.g.*, 0.01–0.29 wt.%; Barkov *et al.* 1995b), although values up to 4.14 wt.% have been reported by Coghill & Wilson (1993), suggesting that the reported Fe is in the structure of braggite.

TABLE 7. ELECTRON-MICROPROBE RESULTS ON TRACE PLATINUM-GROUP ELEMENTS IN SULFIDES, ARSENIDES AND SULFARSENIDES FROM SELECTED SAMPLES OF DRILL CORES R695 AND R713, KEIVITSANSARVI Ni–Cu–PGE DEPOSIT

| PGE | Sample | Mineral | N | >MDL | Ave. | Range |
|------------|--------------|--------------|----|------|---------|---------|
| Rhodium | R713/27.82 | Gersdorffite | 4 | 1 | 41 | <24–41 |
| | R713/40.67 | Gersdorffite | 3 | 1 | 454 | <23–454 |
| | R713/40.90 | Gersdorffite | 5 | 1 | 39 | <23–39 |
| Platinum | R695/84.10 | Pn–Py | 5 | 1 | 42 | <29–42 |
| | R695/84.10 | Chalcopyrite | 4 | 2 | 44 | <27–54 |
| | R695/84.65 | Chalcopyrite | 2 | 1 | 53 | <29–53 |
| | R713/40.90 | Nickeline | 2 | 1 | 36 | <33–36 |
| | R713/27.82 | Gersdorffite | 4 | 1 | 277 | <32–277 |
| | R713/40.90 | Gersdorffite | 5 | 1 | 31 | <30–31 |
| Palladium | R695/84.10 | Pentlandite | 10 | 10 | 113 | 42–150 |
| | R695/84.65 | Pentlandite | 16 | 5 | 23 | <16–27 |
| | R713/40.90 | Pentlandite | 4 | 1 | 19 | <19–19 |
| | R695/84.65 | Pyrite | 3 | 1 | 30 | <16–30 |
| | R695/84.10 | Pn–Py | 5 | 5 | 175 | 111–223 |
| | R695/84.65 | Pn–Py | 5 | 3 | 28 | <15–34 |
| | R695/84.10 | Chalcopyrite | 4 | 1 | 17 | <16–17 |
| | R713/29.2 | Nickeline | 3 | 3 | 155 | 56–342 |
| | R713/40.90 | Nickeline | 2 | 2 | 133 | 47–218 |
| | R713/27.82 | Maucherite | 2 | 2 | 27 | 25–28 |
| | R713/29.2 | Maucherite | 7 | 7 | 95 | 36–241 |
| | R713/27.82 | Gersdorffite | 4 | 4 | 41 | 27–66 |
| | R713/29.2 | Gersdorffite | 4 | 4 | 552 | 196–868 |
| | R713/32.65 | Gersdorffite | 2 | 2 | 392 | 282–501 |
| R713/40.67 | Gersdorffite | 3 | 2 | 225 | <15–259 | |
| R713/40.90 | Gersdorffite | 5 | 4 | 172 | <16–275 | |

N: number of analyses, >MDL: analytical results above minimum detection-limit, Ave: the average of analytical results above minimum detection-limit. Pn–Py: pentlandite–pyrite micro-intergrowth.

Pd antimonides

Six minute grains (<10 μm) of Pd antimonides have been found associated with sulfides, locally isolated, included in hydrous silicates. Most of the analyses have too low or high totals to allow us to discuss their composition properly. Nevertheless, these results indicate the presence of stibiopalladinite or mertieite II (or both), as well as a phase with the formula (Pd_{1.58}Pt_{0.27}Fe_{0.02}Au_{0.02}Os_{0.01})Σ1.9(As_{0.58}Sb_{0.5})Σ1.08, which may represent a Pt- and Sb-rich variety of palladoarsenide (Cabri *et al.* 1975).

Pt–Fe alloy

One minute grain of Pt–Fe alloy (or native platinum) ~5 μm across has been observed included in silicate, together with two other smaller inclusions of sudburyite and sperrylite. Its composition approaches that of isoferroplatinum but is Pt-deficient: (Pt_{2.80}Ni_{0.05}Rh_{0.02}Cu_{0.02}Os_{0.02}Pd_{0.01})Σ2.92Fe_{1.08}.

Gold

The two grains of gold identified are very small (around 6 × 2 μm) and occur included in silicate. Both are very pure, containing only very small amounts of Ag (0.21–0.38 at.%) and Pt (0.2–0.76 at.%). Significant

TABLE 8. REPRESENTATIVE WHOLE-ROCK CONCENTRATIONS OF PLATINUM-GROUP ELEMENTS IN SELECTED SAMPLES FROM DRILL CORES R695 AND R713, KEIVITSANSARVI Ni-Cu-PGE DEPOSIT

| Sample | Os | Ir | Ru | Rh | Pt | Pd | Au | Total PGE | Pt _N /Pd _N | (Pt _N +Pd _N)/Ir _N |
|------------------|----|-----|----|-----|------|-------|-----|-----------|----------------------------------|---|
| R695/80.00-80.50 | 23 | 28 | 35 | 30 | 976 | 614 | 246 | 1951 | 0.85 | 40.62 |
| R695/81.50-82.00 | 20 | 20 | 29 | 19 | 632 | 497 | 107 | 1324 | 0.68 | 41.15 |
| R695/84.00-84.50 | 54 | 30 | 26 | 27 | 9460 | 17000 | 156 | 26597 | 0.30 | 721.20 |
| R695/84.50-85.00 | 29 | 23 | 19 | 23 | 2060 | 2930 | 175 | 5258 | 0.38 | 176.71 |
| R695/85.50-86.00 | 23 | 17 | 17 | 18 | 1430 | 1680 | 68 | 3253 | 0.45 | 141.62 |
| R713/19.00-19.50 | 66 | 17 | 19 | 16 | 8700 | 3220 | 83 | 12121 | 1.44 | 458.61 |
| R713/22.00-22.50 | 78 | 117 | 79 | 133 | 3740 | 934 | 37 | 5118 | 2.14 | 24.83 |
| R713/23.00-23.50 | 8 | 21 | 29 | 23 | 848 | 675 | 126 | 1730 | 0.67 | 52.48 |
| R713/29.00-29.50 | 35 | 115 | 71 | 145 | 5350 | 3530 | 178 | 9424 | 0.81 | 55.04 |
| R713/29.50-30.00 | 18 | 40 | 65 | 41 | 1100 | 683 | 54 | 2001 | 0.86 | 31.32 |
| R713/39.00-39.50 | 24 | 44 | 50 | 47 | 1370 | 1070 | 313 | 2918 | 0.68 | 40.30 |
| R713/40.50-41.00 | 19 | 54 | 70 | 55 | 1790 | 1360 | 242 | 3590 | 0.70 | 42.19 |

Concentrations expressed in ppb.

proportions of Fe (1.39–1.86 at.%) could be the result of contamination from the enclosing silicate.

TRACE PLATINUM-GROUP ELEMENTS IN SULFIDES, ARSENIDES AND SULFARSENIDES

The results of the analyses of trace Ir, Rh, Pt and Pd in sulfides, arsenides and sulfarsenides from the upper section of the Keivitsansarvi Ni-Cu-PGE deposit are listed in Table 7. This table does not include Ir because it has not been detected above the minimum detection-limit (MDL) in any run. These results show that the main carriers of PGE (especially Pd) are gersdorffite and, to a lesser extent, nickeline and maucherite, in agreement with the previous data of Gervilla *et al.* (1997, 1998) and the experimental results of Gervilla *et al.* (1994). Traces of Rh have been detected (up to 454 ppm) in three analyses performed on three different grains of gersdorffite, suggesting that this mineral can dissolve significant amounts of Rh. Traces of Pt have also been found in several analyses performed on different minerals. It has been detected in one analysis of pentlandite-pyrite micro-intergrowths (42 ppm), in three analyses of chalcopyrite (34–54 ppm), in one analysis of nickeline (36 ppm), and in two analyses of gersdorffite (31, 277 ppm). These results show that although minor amounts of Pt can be dissolved in sulfides, arsenides and sulfarsenides, this element is dominantly present in the form of discrete PGM (mainly moncheite and sperrylite). In contrast, Pd minerals are comparatively less abundant than Pt minerals, and Pd tends to occur in the structure of the main ore minerals. As cited above, the main carrier of this PGE is gersdorffite, which usually dissolves several hundred ppm Pd (up to 868 ppm). Similarly, Pd has been detected in all analyses performed on nickeline and maucherite, which contain, respectively, 47–342 ppm and 25–241 ppm Pd. Discrete grains of pentlandite and pentlandite intergrown with

pyrite also carry significant amounts of Pd (<16–150 ppm and <15–223 ppm, respectively). In addition, traces of Pd have been measured in pyrite (30 ppm) and chalcopyrite (17 ppm). However, the latter result is only slightly above the minimum detection-limit.

WHOLE-ROCK CONTENTS OF NOBLE METALS

The results of whole-rock noble-metal analyses (Table 8) show that the samples studied contain high amounts of PGE, ranging between 1323 and 26597 ppb (total PGE), but low gold (32–313 ppb). At the scale of the drill-cores samples, these values are not correlated with concentrations of S, As, Ni, Cu or Cl, in spite of the general correlation described by Mutanen (1997) at an intrusion scale.

Chondrite-normalized patterns of the various samples are relatively similar, with Os, Ir and Ru between 0.01 and 0.1 times chondritic values, followed by positive slopes from Ru to Pd (up to thirty times chondritic values), and either a slight enrichment or a strong depletion in Au (Fig. 7). Only three samples from drill core R713 deviate from this general pattern, showing positive Pt anomalies relative to Pd. The fact that the Pd:Pt ratio is generally above unity, in spite of the predominance of Pt minerals in the ore assemblage, further confirms that most of the Pd is hidden in solid solution in gersdorffite, nickeline, maucherite and pentlandite. However, the most important differences appear in Ir, Ru and, to a lesser extent, Os, which are enriched in arsenide-bearing samples but not correlated with total As. Thus in the arsenide-free samples from drill core R695, most of these elements are concentrated between 0.02 and 0.05 times chondritic values and show nearly flat or slightly negatively sloped chondrite-normalized patterns. Similarly, the four shallowest and three other arsenide-poor samples from drill core R713 display low Ir and Ru contents (between 0.02 and 0.04 times chon-

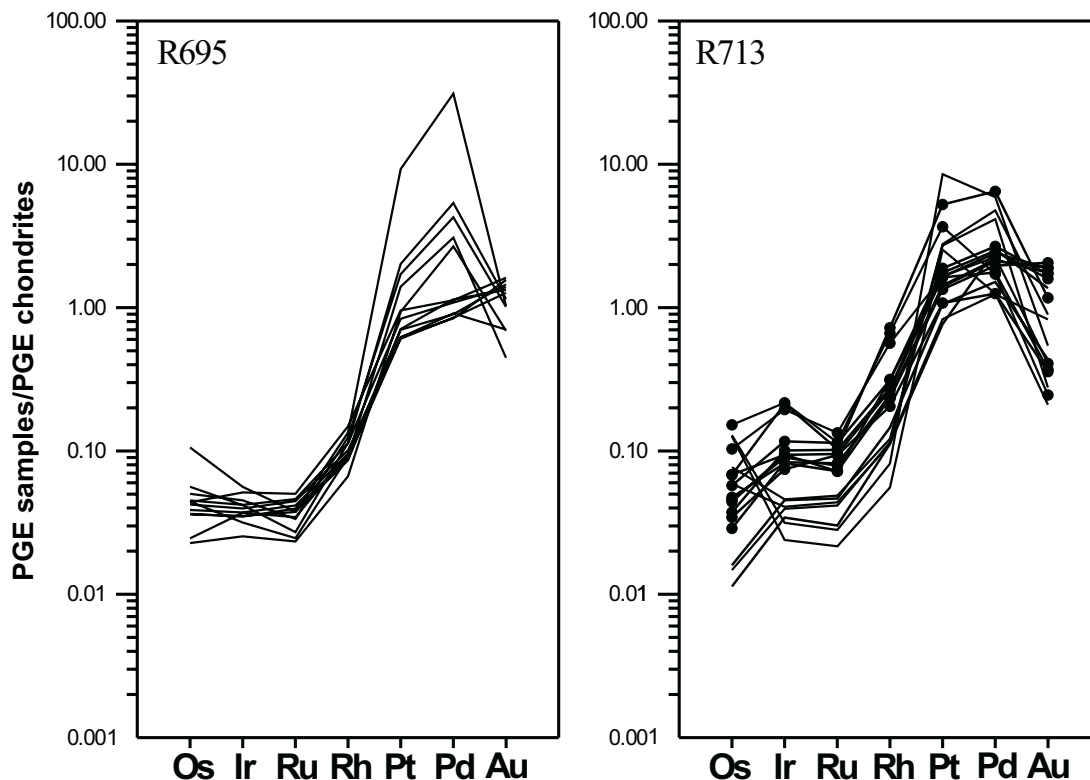


Fig. 7. Chondrite-normalized PGE diagrams of samples from drill cores R695 and R713, representative of the upper part of the Keivitsansarvi deposit. Patterns marked with dots represent samples containing arsenides and sulfarsenides.

ditric values), with variable levels of Os. In arsenide-rich samples, Ir and Ru contents increase up to 0.2 times chondritic values (Fig. 7). These data show a close correlation between arsenides and the more refractory PGE. Although we have not observed any PGM containing these elements in the samples studied, the presence of composite sulfarsenide crystals containing a core of irarsite surrounded by hollingworthite and cobaltite in heavy concentrates from other drill cores of the Keivitsa intrusion and in disseminated sulfide ores of the Satovaara intrusion (Mutanen 1997) suggests that these sulfarsenides could be the carriers of Ir, Rh and, to a lesser extent, Os and Ru in the Keivitsansarvi deposit.

PGE values in the upper section of the Keivitsansarvi deposit (Table 8) are, on the whole, ten times higher than those reported by Mutanen (1997) for Ni-PGE ores. Furthermore, the reported average concentrations of Pt (1734 ppb in drill core R695 and 2377 ppb in R713) and Pd (2428 ppb in drill core R695 and 1472 ppb in R713) approach those of some reef-type PGE deposits like the Sompujärvi (sulfide-type) reef and the Ala-Penikka (normal) reef in the Penikat layered intrusion (Halkoaho *et al.* 1990a, b), and the Merensky Reef in

the Bushveld Complex (Barnes *et al.* 1985), which contain, respectively, 2667 ppb, 1965 ppb and 3740 ppb Pt, and 2700 ppb, 7125 ppb and 1530 ppb Pd, on average. These data suggest that the section studied represents a PGE-enriched horizon. There may be significant economic potential to the Keivitsansarvi deposit.

DISCUSSION

Mineralogical and textural relations of the Keivitsansarvi PGM show evidence that, although some of these phases could have crystallized at a magmatic temperature (*e.g.*, those that remain included in cumulus silicates), most of them formed or re-equilibrated at moderately low-temperature conditions. The fact that most of these grains occur included in hydrous silicates or at the contacts between sulfides and silicates indicates that late magmatic, hydrothermal or metamorphic processes had to play an important role in the genesis of these PGM.

Moncheite is stable up to 1150°C (Elliot 1965); however, the compositional trend shown by the grains we analyzed (Figs. 3, 4), with extensive substitution of Te

for Bi and of Pt for Pd, suggests a lower temperature of formation. Although no experimental data are available in the systems Pt–Pd–Te and Pt–Bi–Te, this suggestion is in agreement with the low thermal stability of PdTe₂ (752°C: Kim *et al.* 1990) and α -PdBi₂ (420°C: Shunk 1969). Merenskyite thus had to crystallize well below magmatic temperatures. Although it could be argued that the high Pt content of the merenskyite we analyzed should increase its thermal stability (752°C: Kim *et al.* 1990), Hoffman & MacLean (1976) showed that the stability of this mineral strongly decreases with the substitution of Te for Bi. The kotulskite end-member of the kotulskite – sobolevskite – (sudburyite) solid-solution series decomposes at 746°C (Kim *et al.* 1990) but, probably, this limit of thermal stability diminishes with the substitution of Te for Bi, as occurs in merenskyite. Michenerite is stable only below 500°C (Hoffman & MacLean 1976).

According to the experimental results in the system PtS–PdS–NiS (Verryn & Merkle 2002), the analyzed grain of cooperite crystallized around 950°C, and its composition does not reflect equilibrium with the only grain of braggite found. The chemical composition of the latter plots outside the compositional fields established by Verryn & Merkle (2002) between 1200° and 700°C. According to these experimental results, the solubility of Ni in braggite tends to increase as temperature decreases, which suggests that our analyses could correspond to a mineral equilibrated below 700°C. The reported composition of braggite is similar to that from the Lukkulaivaara layered intrusion, which crystallized below 600°C (Barkov *et al.* 1995b). Nevertheless, an alternative interpretation of Pd–Pt(\pm Ni) sulfides whose compositions plot inside the miscibility gap between braggite and cooperite established experimentally (Verryn & Merkle 2002) is that they are metastable phases resulting from the loss of Pd during hydrothermal alteration (R.K.W. Merkle, pers. commun., 2001). The preferential leaching of Pd could be explained by the lower stability of PdS, compared to PtS, in aqueous solutions under different thermodynamic conditions (Gammons *et al.* 1992, Wood *et al.* 1992). The Pd-impooverished altered grains should preserve their original (braggite) structure (*e.g.*, Barkov *et al.* 1995b).

The texture of the sulfide assemblages described can be interpreted on the basis of phase relations in the system Fe–Ni–S at 725°C (Karup-Møller & Makovicky 1995), 650°C (Kullerud *et al.* 1969), 400°C (Craig *et al.* 1968) and 230°C (Misra & Fleet 1973). These experimental results predict that Ni-rich pyrite formed slightly above 725°C in equilibrium with monosulfide solid-solution (*mss*) and Fe-rich vaesite (NiS₂) or with *mss* alone for Fe-richer compositions. On cooling, Fe-rich vaesite became unstable for the average bulk-composition of pentlandite–pyrite assemblages (~54–59 at.% S, ~29–30% Fe and ~10–12% Ni; estimated from chalcopyrite-free composite aggregates of coexisting pyrite and pentlandite) and upon reaching 400°C, re-

acted with the coexisting *mss* to form a *mss* richer in Ni in equilibrium with Ni-rich pyrite. As temperature continued to drop, Ni-rich *mss* decomposes, forming pyrite and pentlandite at 230°C. This reaction sequence explains the abundance of fine pyrite–pentlandite intergrowths in the polished sections studied. Slight variations in the bulk composition of the original, interstitial sulfide melt gave rise to different proportions of pyrite and pentlandite showing the diverse textures described. In addition, the presence of chalcopyrite in many interstitial aggregates of sulfides indicates that this mineral could be in equilibrium with pyrite and intermediate solid-solution (*iss*) when it becomes stable at 557°C (Cabri 1973). On cooling, this ternary assemblage changes to chalcopyrite – pyrite – pyrrhotite. This conversion could explain the presence of euhedral crystals of pyrite in chalcopyrite and of pyrite–chalcopyrite intergrowths. However, the common absence of monoclinic pyrrhotite in these assemblages, as well as the presence of monoclinic pyrrhotite associated to intergrown pentlandite and pyrite, suggest that other factors (*e.g.*, hydrothermal alteration, metamorphism) modified the expected low-temperature phase relations, giving rise to non-equilibrium assemblages.

The above-described evolutionary picture of the disseminated Ni–Cu mineralization, formed by intercumulus crystallization of a small fraction of immiscible sulfide melt, is somewhat different in arsenide-rich samples from drill core R713. Experimental results on the partitioning of platinum-group elements in the system Fe–Ni–Cu–S (containing minor amounts of As, Te and Bi: Fleet *et al.* 1993), as well as the textural relations of nickeline and maucherite with sulfide aggregates, suggest that these minerals could have formed later during the crystal fractionation of the sulfide melt, together with chalcopyrite and *iss*. On cooling, nickeline and maucherite reacted with the coexisting sulfides to form gersdorffite coronae around Ni arsenides or discrete crystals where the amount of arsenides was very small. The compositional trend shown by gersdorffite indicates that it could start to crystallize around 500°C (for the Co-richer compositions, Klemm 1965), but re-equilibrated on cooling by the substitution of Co for Ni, under moderately high anion (S and As) fugacities (Hem *et al.* 2001).

Although most textural relations can be ascribed to this magma-related magma-related mineralization upon cooling, the low thermal stability of the bismuthotellurides associated to hydrous silicates, the composition of Pd–Pt(\pm Ni) sulfides and the presence of non-equilibrium assemblages in the sulfides clearly indicate the activity of fluids. Our present knowledge does not allow us to establish unequivocally the nature of such fluids nor the timing of a possible hydrothermal event related to low-density fluids separated from the crystallizing intercumulus melt (such as those described by Boudreau & McCallum 1992). It is evident, however, that the rocks of the upper section of the

Keivitsansarvi deposit suffered partial serpentinization followed by metamorphism under greenschist-facies conditions, associated to extensive hydrothermal alteration (Tyrväinen 1983, P. Hölttä, pers. commun.). Serpentinization caused Ni release from olivine, since lizardite does not contain much of this element (Barnes & Hill 2000) and, consequently, Ni was collected by the coexisting sulfides, which favored the stabilization of Ni-rich assemblages containing pentlandite and millerite (Eckstrand 1975, Barnes & Hill 2000). In arsenide-bearing assemblages, serpentinization could cause partial loss of As, stabilizing maucherite-bearing (Ni-rich) assemblages. Hydrothermal alteration associated with metamorphism could remobilize PGE, probably in the form of chloride complexes (the host rocks of the Keivitsansarvi deposit are very rich in Cl; Mutanen 1997), and precipitate them in discrete horizons. PGE-rich ores do not constitute a single, continuous horizon (as should be expected from magmatic crystallization), but form discontinuous bands at variable depths. Three-dimensional modeling of PGE distribution and preliminary analytical data on other drill cores (with Pt and Pd reaching up to 2640 and 1160 ppb, respectively) provide evidence for the presence of several PGE-enriched horizons in the upper section of the Keivitsansarvi deposit. The hydrothermal fluids carried some arsenic (and other semimetals), as the existence of a second generation of maucherite replacing gersdorffite along the outer boundary of grains shows. Consequently, metamorphism of the host mafic-ultramafic rocks partly dissolved the sulfide (and arsenide) aggregates, as well as the PGM, but mostly redistributed them. That is why these minerals generally occur intersected by late amphibole, antigorite and chlorite, along cleavage planes of the hydrous silicates, and fill late fractures and veins. During this process, disseminated sulfides recrystallized and re-equilibrated with olivine, resulting in further enrichment of Ni in the sulfides (*e.g.*, Barnes & Hill 2000, Mancini & Papunen 2000).

During the magmatic crystallization of the sulfide ore, most of the Pt was concentrated in discrete minerals, whereas Pd behaved according to its crystal-chemical affinity during the fractional crystallization of the sulfide melt (Makovicky *et al.* 1986, Gervilla *et al.* 1994). Thus, Pd entered the structure of moncheite at high temperature and formed other Pd tellurides, arsenides and antimonides on cooling. Nevertheless, a major part of Pd partitioned, in arsenide-free samples, into the *mss* and was accommodated in the pentlandite structure as it crystallized. In arsenide-bearing samples, Pd was fractionated with As to the residual Cu-rich sulfide melt, and was collected by the crystallizing nickeline and maucherite, and later, entered the structure of gersdorffite. The stabilization of both pentlandite and maucherite during serpentinization, preserved (and could even increase) the Pd content of these minerals (Makovicky *et al.* 1986, Gervilla *et al.* 1994). The metamorphism associated with hydrothermal alteration

of the ores resulted in the remobilization of PGM followed by their re-equilibration and precipitation in geochemically favorable horizons, and in the redistribution of Pd minerals combined with intercumulus hydrous silicates and arsenides, especially high-Pd gersdorffite.

ACKNOWLEDGEMENTS

The authors dedicate this paper to Louis J. Cabri on the occasion of his official retirement. It is clear that although retired, he will continue to be a leader in the investigation of PGE-enriched assemblages in ores. In this respect, Dr. Cabri tested the electron-microprobe-derived trace-PGE results on sulfides and arsenides by comparing them with PIXE data; a collaborative paper is now in preparation. The authors thank the Geological Survey of Finland for permission to publish this paper, and the Junta de Andalucía (Research Group No. 4028) for partial financial support. Mr. Bo Johanson kindly assisted in the electron-probe micro-analyses. Constructive comments of H. O'Brien, T.A.A. Halkoaho, R.K.W. Merkle, A.Y. Barkov and R.F. Martin improved this contribution significantly. This paper is a contribution to IGCP Project No 427.

REFERENCES

- ALAPIETI, T.T., FILÉN, B.A., LAHTINEN, J.J., LAVROV, M.M., SMOLKIN, V.F. & VOITSEKHOVSKY, S.N. (1990): Early Proterozoic layered intrusions in the northeastern part of the Fennoscandian Shield. *Mineral. Petrol.* **42**, 1-22.
- AUGÉ, T., LEGENDRE, O. & MAURIZOT, P. (1998): The distribution of Pt and Ru–Os–Ir minerals in the New Caledonia ophiolite. In *International Platinum* (N.P. Laverov & V.V. Distler, eds.). Theophrastus, St.-Petersburg, Russia (141-154).
- BARKOV, A.Y., MARTIN, R.F., TARKIAN, M., POIRIER, G. & THIBAUT, Y. (2001): Pd–Ag tellurides from a Cl-rich environment in the Lukkulaivaara layered intrusion, northern Russian Karelia. *Can. Mineral.* **39**, 639-654.
- _____, PAKHOMOVSKII, Y.A. & MEN'SHIKOV, Y.P. (1995b): Zoning in the platinum-group sulfide minerals from the Lukkulaivaara and Imandrovsky layered intrusions, Russia. *Neues Jahrb. Mineral., Abh.* **169**, 97-117.
- _____, SAVCHENKO, Y.E. & ZHANGUROV, A.A. (1995a): Fluid migration and its role in the formation of platinum-group minerals: evidence from the Imandrovsky and Lukkulaivaara layered intrusions, Russia. *Mineral. Petrol.* **54**, 249-260.
- BARNES, S.J. & HILL, R.E.T. (2000): Metamorphism of komatiite-hosted nickel sulfide deposits. *Rev. Econ. Geol.* **11**, 203-215.
- _____, NALDRETT, A.J. & GORTON, M.P. (1985): The origin of the fractionation of platinum-group elements in terrestrial magmas. *Chem. Geol.* **53**, 303-323.

- BOUDREAU, A.E. & MCCALLUM, I.S. (1992): Concentration of platinum-group elements by magmatic fluids in layered intrusions. *Econ. Geol.* **87**, 1830-1848.
- CABRI, L.J. (1973): New data on phase relations in the Cu-Fe-S system. *Econ. Geol.* **68**, 443-454.
- _____, HARRIS, D.C. & WEISER, T.W. (1996): Mineralogy and distribution of platinum-group mineral (PGM) in placer deposits of the world. *Explor. Mining Geol.* **5**, 73-167.
- _____, LAFLAMME, J.H.G., STEWART, J.M., ROWLAND, J.F. & CHEN, T.T. (1975): New data on some palladium arsenide and antimonides. *Can. Mineral.* **13**, 321-335.
- _____, _____, _____, TURNER, K. & SKINNER, B.J. (1978): On cooperite, braggite and vvsotskite. *Am. Mineral.* **63**, 832-839.
- COGHILL, B.M. & WILSON, A.H. (1993): Platinum-group minerals in the Selukwe Subchamber, Great Dyke, Zimbabwe: implications for PGE collection mechanisms and post-formational redistribution. *Mineral. Mag.* **57**, 613-633.
- COUSENS, D.R., RASCH, R. & RYAN, C.G. (1997): Detection limits and accuracy of the electron and proton microprobe. *Micron* **28**, 231-239.
- CRAIG, J.R., NALDRETT, A.J. & KULLERUD, G. (1968): The 400°C isothermal diagram Fe-Ni-S. *Carnegie Inst. Wash., Year Book* **66**, 440-441.
- ECKSTRAND, O.R. (1975): The Dumont serpentinite: a model for control of nickeliferous opaque assemblages by alteration products in ultramafic rocks. *Econ. Geol.* **70**, 183-201.
- ELLIOT, R.P. (1965): *Constitution of Binary Alloys (1st Supplement)*. McGraw-Hill, New York, N.Y.
- EVSTIGNEEVA, T.L., GENKIN, A.D. & KOVALENKER, V.A. (1976): Sobolevskite, a new bismuthide of palladium, and the nomenclature of minerals of the system PdBi-PdTe-PdSb. *Int. Geol. Rev.* **18**, 856-866.
- FLEET, M.E., CHRYSOULIS, S.L., STONE, W.E. & WEISNER, C.G. (1993): Partitioning of platinum-group elements and Au in the Fe-Ni-Cu-S system: experiments on the fractional crystallization of sulfide melt. *Contrib. Mineral. Petrol.* **115**, 36-44.
- GAMMONS, C.H., BLOOM, M.S. & YU, Y. (1992): Experimental investigation of the hydrothermal geochemistry of platinum and palladium. I. Solubility of platinum and palladium sulfide minerals in NaCl/H₂SO₄ solutions at 300°C. *Geochim. Cosmochim. Acta* **56**, 3881-3894.
- GERVILLA, F., MAKOVICKY, E., MAKOVICKY, M. & ROSE-HANSEN, J. (1994): The system Pd-Ni-As at 790°C and 450°C. *Econ. Geol.* **89**, 1630-1639.
- _____, PAPUNEN, H., KOJONEN, K. & JOHANSON, B. (1997): Results of trace platinum group element analyses of arsenides and sulfarsenides from some Finnish PGE-bearing mafic-ultramafic intrusions. In *Mineral Deposits: Research and Exploration, Where Do They Meet?* (H. Papunen, ed.). Balkema, Rotterdam, The Netherlands (423-426).
- _____, _____, _____ & _____ (1998): Platinum-, palladium- and gold-rich arsenide ores from the Kylmäkoski Ni-Cu deposit (Vammala Nickel Belt, SW Finland). *Mineral. Petrol.* **64**, 163-185.
- GRATEROL, M. & NALDRETT, A.J. (1971): Mineralogy of the Marbridge No. 3 and no. 4 nickel-iron sulfide deposits, with some comments on low-temperature equilibration in the Fe-Ni-S system. *Econ. Geol.* **66**, 886-900.
- HALKOaho, T.A.A., ALAPIETI, T.T. & LAHTINEN, J.J. (1990a): The Sompujärvi PGE reef in the Penikat layered intrusion, northern Finland. *Mineral. Petrol.* **42**, 39-56.
- _____, _____, _____ & LERSSI, J.M. (1990b): The Ala-Penikka PGE reefs in the Penikat layered intrusion, northern Finland. *Mineral. Petrol.* **42**, 23-38.
- HANSKI, E.J., GRINENKO, L.N. & MUTANEN, T. (1996): Sulfur isotopes in the Keivitsa Cu-Ni-bearing intrusion and its country rocks, northern Finland: evidence for crustal sulfur contamination. In *IGCP Project 336 Symposium (Rovaniemi, Finland). Program and Abstr., Univ. of Turku, Div. Geol. Mineral., Publ.* **33**, 15-16.
- HARNEY, D.M.W. & MERKLE, R.K.W. (1990): Pt-Pd minerals from the upper zone of the eastern Bushveld Complex, South Africa. *Can. Mineral.* **28**, 619-628.
- HEM, S.R., MAKOVICKY, E. & GERVILLA, F. (2001): Compositional trends in Fe, Co and Ni sulfarsenides and their crystal-chemical implications: results from the Arroyo de la Cueva deposits, Ronda Peridotite, southern Spain. *Can. Mineral.* **39**, 831-853.
- HOFFMAN, E. & MACLEAN, W.H. (1976): Phase relations of michenerite and merenskyite in the Pd-Bi-Te system. *Econ. Geol.* **71**, 1461-1468.
- HUHMA, H., MUTANEN, T., HANSKI, E., RÄSÄNEN, J., MANNINEN, T., LEHTONEN, M., RASTAS, P. & JUOPPERI, H. (1996): Isotopic evidence for contrasting sources of the prolonged Palaeoproterozoic mafic-ultramafic magmatism in central Finnish Lapland. In *IGCP Project 336 Symposium (Rovaniemi, Finland). Program and Abstr., Univ. of Turku, Div. Geol. Mineral., Publ.* **33**, 17.
- _____, _____, _____ & WALKER, R. (1995): Sm-Nd, U-Pb and Re-Os isotopic study of the Keivitsa Cu-Ni bearing intrusion, northern Finland. In *The 22nd Nordic Geological Winter Meeting (Turku, Finland), Abstr. Book*, 72.
- HUHTELIN, T.A., ALAPIETI, T.T. & LAHTINEN, J.J. (1990): The Paasivaara PGE reef in the Penikat layered intrusion, northern Finland. *Mineral. Petrol.* **42**, 57-70.
- ILJINA, M. (1994): The Portimo layered igneous complex, with emphasis on diverse sulphide and platinum-group element deposits. *Acta Universitatis Ouluensis A* **258**.

- JOHANSON, B. & KOJONEN, K. (1995): Improved electron probe microanalysis services at Geological Survey of Finland. *Geol. Surv. Finland, Spec. Pap.* **20**, 181-184.
- _____ & _____ (1996): Results of major and trace element analyses of kimberlitic garnet. *EMAS'96 workshop (Balatonfűrhed, Hungary), Poster Abstr.*
- JUVONEN, R., KALLIO, E. & LAKOMAA, T. (1994): Determination of precious metals in rocks by inductively coupled plasma mass spectrometry using nickel sulfide concentration. Comparison with other pre-treatment methods. *Analyst* **119**, 617-621.
- KARUP-MØLLER, S. & MAKOVICKY, E. (1995): The phase system Fe-Ni-S at 725°C. *Neues Jahrb. Mineral., Monatsh.*, 1-10.
- KIM, WON-SA, CHAO, G.Y. & CABRI, L.J. (1990): Phase relations in the Pd-Te system. *J. Less-Common Metals* **162**, 61-74.
- KLEMM, D.D. (1965): Synthesen und Analysen in den Dreieckdiagrammen FeAsS-CoAsS-NiAsS und FeS₂-CoS₂-NiS₂. *Neues Jahrb. Mineral., Abh.* **103**, 205-255.
- KOJONEN, K. & JOHANSON, B. (1999a): Trace EPMA of nickel in kimberlitic garnet, gold and PGE in sulfides and arsenides. *MINSA Mini-Symp. 16. Council of Geosciences, Pretoria, South Africa, Extended Abstr. Vol.*, 96-99.
- _____ & _____ (1999b): Determination of refractory gold distribution by microanalysis, diagnostic leaching and image analysis. *Mineral. Petrol.* **67**, 1-19.
- _____, _____ & GERVILLA, F. (1998): Electron microprobe analysis of trace Pt and Pd: examples of arsenides and sulfarsenides. *8th Int. Platinum Symp. (Rustenburg), Abstr. Vol.*, 175-178.
- KULLERUD, G., YUND, R.A. & MOH, G.H. (1969): Phase relations in the Cu-Fe-S, Cu-Ni-S, and Fe-Ni-S systems. *Econ. Geol., Monogr.* **4**, 323-343.
- LEGENDRE, O. & AUGÉ, T. (1992): Alluvial platinum-group minerals from the Manampotsy area, East Madagascar. *Aust. J. Earth Sci.* **39**, 389-404.
- MAKOVICKY, M., MAKOVICKY, E. & ROSE-HANSEN, J. (1986): Experimental studies on the solubility and distribution of platinum group elements in base-metal sulfides in platinum deposits. In *Metallogeny of Basic and Ultrabasic Rocks* (M.J. Gallagher, R.A. Ixer, C.R. Neary & H.M. Prichard, eds.). Inst. Mining Metallurgy, London, U.K. (415-425).
- MANCINI, F. & PAPUNEN, H. (2000): Metamorphism of Ni-Cu sulfides in mafic-ultramafic intrusions: the Svecofennian Sääksjärvi complex, southern Finland. *Rev. Econ. Geol.* **11**, 217-231.
- MISRA, K.C. & FLEET, M.E. (1973): The chemical composition of synthetic and natural pentlandite assemblages. *Econ. Geol.* **68**, 518-539.
- MOSTERT, A.B., HOFMEYER, P.K. & POTGIETER, G.A. (1982): The platinum group mineralogy of the Merensky Reef at the Impala platinum mines, Bophuthatswana. *Econ. Geol.* **77**, 1385-1394.
- MUTANEN, T. (1997): Geology and ore petrology of the Akanvaara and Koitelainen mafic layered intrusions and the Keivitsa-Satovaara layered complex, northern Finland. *Geol. Surv. Finland, Bull.* **395**.
- _____, TÖRNROOS, R. & JOHANSON, B. (1988): The significance of cumulus chlorapatite and high-temperature dashkesanite to the genesis of PGE mineralization in the Koitelainen and Keivitsa-Satovaara complexes, northern Finland. In *Geoplatinum 87* (H.M. Prichard, P.J. Potts, J.F.W. Bowles & S.J. Cribb, eds.) Elsevier, London, U.K. (159-160).
- POUCHOU, J.-L. & PICOIR, F. (1984): A new model for advanced X-ray microanalysis. *La Recherche Aérospatiale* **3**, 167-192.
- ROBINSON, B.W. & GRAHAM, J. (1992): Advances in electron microprobe trace-element analysis. *J. Computer-Assisted Microsc.* **4**(3).
- _____, WARE, N.G. & SMITH, D.G.W. (1998): Modern electron-microprobe trace-element analysis in mineralogy. In *Modern Approaches of Ore and Environmental Mineralogy* (L.J. Cabri & D.J. Vaughan, eds.). *Mineral. Assoc. Can., Short Course* **27**, 153-180.
- SHUNK, F.A. (1969): *Constitution of Binary Alloys (2nd Supplement)*. McGraw-Hill, New York, N.Y.
- TYRVÄINEN, A. (1983): *Pre-Quaternary Rocks of the Sodankylä and Sattanen Map-Sheet Areas, Sheet 3713 and 3714*. Geological Survey of Finland, Espoo, Finland (in Finnish with English summary).
- VERRYN, S.M.C. & MERKLE, R.K.W. (2000): Synthetic "cooperite", "braggite" and "vysotskite" in the system PtS-PdS-NiS at 1100°C, 1000°C and 900°C. *Mineral. Petrol.* **68**, 63-73.
- _____ & _____ (2002): The system PtS-PdS-NiS between 1200° and 700°C. *Can. Mineral.* **40**, 571-584.
- VOLBORTH, A., TARKIAN, M., STUMPFL, E.F. & HOUSLEY, R.M. (1986): A survey of the Pd-Pt mineralization along the 35-km strike of the J-M Reef, Stillwater Complex, Montana. *Can. Mineral.* **24**, 329-346.
- WALKER, R.K. (1990): *TURBO-SCAN, the Rare-Phase Locating System*. Department of Mineral Resources Engineering, Royal School of Mines, Imperial College, London, U.K.
- WEISER, T.W., OBERTHÜR, T., KOJONEN, K. & JOHANSON, B. (1998): Distribution of trace PGE in pentlandite and of PGM in the Main Sulfide Zone (MSZ) at Mimosa mine, Great Dyke, Zimbabwe. *8th Int. Platinum Symp. (Rustenburg), Abstr. Vol.*, 443-445.

WOOD, S.A., MOUNTAIN, B.W. & PAN, PUJING (1992): The aqueous geochemistry of platinum, palladium and gold: recent experimental constraints and a re-evaluation of theoretical predictions. *Can. Mineral.* **30**, 955-982.

ZIEBOLD, T.O. (1967): Precision and sensitivity in electron microprobe analysis. *Anal. Chem.* **39**, 858-861.

Received September 28, 2000, revised manuscript accepted December 17, 2001.

APPENDIX: SAMPLES AND ANALYTICAL METHODS

The samples used for this study were selected from two different drill cores (R695 and R713) with an aim to collect representative material from the upper section of the Keivitsansarvi Ni–Cu–PGE–Au deposit where, according to Mutanen (1997), platinum-group elements (PGE) are concentrated. The samples were taken in lengths of 20–50 cm from the drill cores.

Electron-probe micro-analysis

The mineralogy and texture of the PGM, sulfides as well as their relations with the associated silicates, were investigated in polished sections and polished thin sections by both reflected- and transmitted-light microscopy, systematic scanning electron microscopy (SEM) in back-scattered electron image mode (BEI) and energy-dispersion spectroscopy (EDS) analyses for rapid identification followed by quantitative wavelength-dispersion spectrum (WDS) electron-microprobe analyses.

The electron-microprobe analyses were done at the Geological Survey of Finland using a Cameca SX50 instrument (Johanson & Kojonen 1995). The platinum-group minerals (PGM) were located automatically in the polished sections using the TURBO-SCAN rare-phase search program (Walker 1990), which is based on the brightness of the back-scattered electron (BSE) signal from heavy phases exceeding 1 μm in size. Normally, six round 2.5-cm polished sections were scanned overnight; the following morning, the PGM were relocated according to the coordinates listed by the program, analyzed by EDS and, where large enough, by WDS for quantitative analysis. Each PGM grain was photographed with the PGT Imix image-analysis program for documentation and grain-size analysis. WDS analyses used an accelerating voltage of 15 kV and probe current of 20 nA for PGM and 20 kV and 45 nA for sulfides. The analytical lines and crystals used for the platinum-group elements were: PtL α on LiF, OsM α on TAP, PdL α , IrM α , RuL α and RhL α on PET. The selection of analytical X-ray lines, background-measurement positions and analyzing crystals was planned to eliminate the inter-element peak overlaps of different PGE. Standards for PGE were metallic Pt, Pd, Os, Ir, Rh and Ru. Other standards were: HgS for Hg, pentlandite for Fe and Ni, pyrite for S, chalcopyrite for Cu, cobaltite for Co and As, Bi₂Se₃ for Bi and Se, metallic Ag and Sb₂Te₃

for Sb and Te. The Cameca software applies the PAP data correction method (Pouchou & Pichoir 1984).

Although it is generally considered that the electron microprobe cannot be used for trace-element analysis, detection limits of 5–20 ppm are routinely achieved (Cousens *et al.* 1997, Gervilla *et al.* 1997, 1998, Robinson *et al.* 1998). Even sub-ppm detection limits have been achieved for favorable elements (*e.g.*, Si, Ti, Cr) using higher currents and longer counting times than normally used in major-element analysis (Robinson *et al.* 1998). Trace analyses of Ni in silicates, Au in pyrite and arsenopyrite and PGE in sulfides, arsenides and sulfarsenides have recently been done at the Geological Survey of Finland using the Australian CSIRO-Trace analysis program specially designed for the Cameca SX50 (Johanson & Kojonen 1995, 1996, Kojonen *et al.* 1998, Weiser *et al.* 1998, Kojonen & Johanson 1999a, b). The conditions of analysis in trace analysis of PGE were: accelerating voltage 35 kV, probe current 500 nA, measuring time 600 s (300 s for peak, 150 s for background on both sides of the peak); metallic standards Pt, Pd, Ru, Ir; analysis lines PtL α , PdL α , RuL α , IrM α ; analysis crystals: LiF for Pt, TAP for Ir, PET for Pd, Rh. The statistical standard deviations (σ) calculated by the CSIRO-Trace program for these analyses were 9–14 ppm, corresponding to minimum detection limits (2σ , 95% confidence) of 18 to 28 ppm. In this study, the pure PGE metals were used as standards and measured with the same accelerating voltage as the sample, but with a smaller sample current (*ca.* 10 nA) to avoid detector deadtime problems. The detection limits calculated from the pure element peak/background measurements according to the Ziebold equation (Ziebold 1967) correspond roughly to twice the standard deviation of the trace-element measurements by the CSIRO-Trace program. The calculated limits of detection are: 30–34 ppm Pt, 24–28 ppm Ru, 20–22 ppm Ir and 18–20 ppm Pd.

For trace-element analysis using an electron microprobe, it is necessary to study the background carefully around the trace-element X-ray lines of interest to find out the shape of the background and possible overlaps of minor peaks from other elements present in the sample. This may be done using the Spectrum-Scan program of the CSIRO-Trace program package using predefined step-lengths and dwell-times. In some cases,

the background shape may be concave, convex or inclined. The background positions were determined from the target minerals using the above mentioned procedure and measured on both sides of the lines ($PtL\alpha$, $PdL\alpha$, $RhL\alpha$ and $IrM\alpha$). The results of the scans were plotted in x - y diagrams to determine the background offsets on both sides of the peak.

The final minimum limit of detection depends on number of counts on peak and background, the peak-to-background ratio, and the X-ray excitation efficiency, which depend on the characteristics of the diffraction crystals. The detection limit is strongly dependent on the accelerating voltage used, especially with the LIF crystal (Robinson & Graham 1992). For TAP and PET

crystals, the improvement of the detection limit is not so large with increasing accelerating voltage.

Platinum-group-element and whole-rock analysis

The drill-core samples were crushed and ground for the inductively coupled plasma – mass spectrometry (ICP–MS) and X-ray-fluorescence (XRF) analysis (Juvonen *et al.* 1994). For the ICP–MS analyses, the PGE and Au were preconcentrated by nickel sulfide fire assay before analysis. The XRF analyses for the major elements were done on powder pellets using a fundamental parameter correction program developed in the Research Laboratory of the Rautaruukki Company, Raahé, Finland, by Mr. Ilmari Alavainio.